

## Proteomics Strategy to Identify Substrates of LNX, a PDZ Domain-containing E3 Ubiquitin Ligase

Zhengguang Guo,<sup>†,‡</sup> Eli Song,<sup>\*,‡,§</sup> Sucas Ma,<sup>†</sup> Xiaorong Wang,<sup>†</sup> Shijuan Gao,<sup>†</sup> Chen Shao,<sup>†</sup> Siqu Hu,<sup>†</sup> Lulu Jia,<sup>†</sup> Rui Tian,<sup>†</sup> Tao Xu,<sup>§</sup> and Youhe Gao<sup>\*,†</sup>

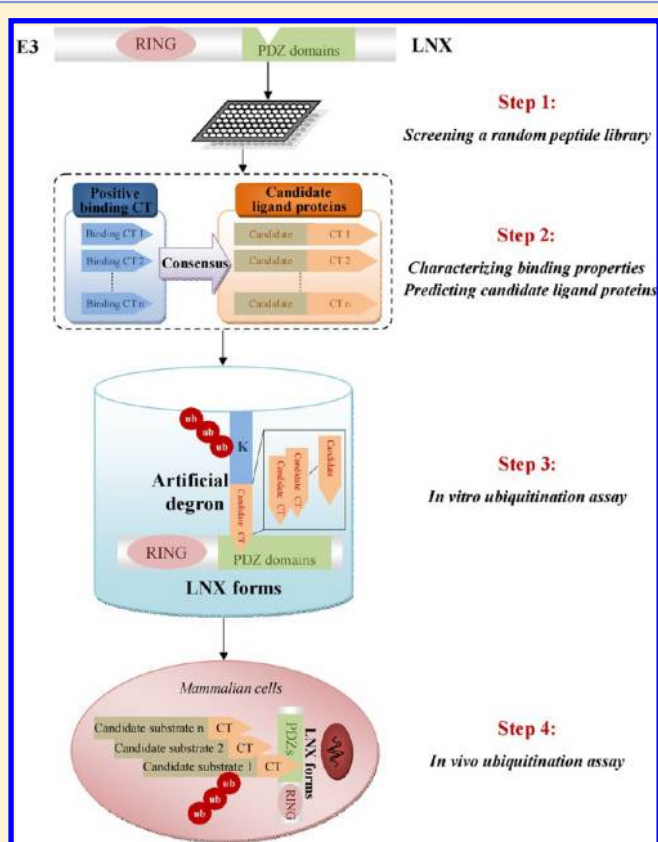
<sup>†</sup>National Key Laboratory of Medical Molecular Biology, Department of Physiology and Pathophysiology, Institute of Basic Medical Sciences, Chinese Academy of Medical Sciences/School of Basic Medicine, Peking Union Medical College, Beijing 100005, China

<sup>§</sup>National Key Laboratory of Biomacromolecules, Institute of Biophysics, Chinese Academy of Sciences, Beijing 100101, China

### **S** Supporting Information

**ABSTRACT:** Ubiquitin ligases (E3s) confer specificity to ubiquitination by recognizing target substrates. However, the substrates of most E3s have not been extensively discovered, and new methods are needed to efficiently and comprehensively identify these substrates. Mostly, E3s specifically recognize substrates via their protein interaction domains. We developed a novel integrated strategy to identify substrates of E3s containing protein interaction domains on a proteomic scale. The binding properties of the protein interaction domains were characterized by screening a random peptide library using a yeast two-hybrid system. Artificial degrons, consisting of a preferential ubiquitination sequence and particular interaction domain-binding motifs, were tested as potential substrates by *in vitro* ubiquitination assays. Using this strategy, not only substrates but also nonsubstrate regulators can be discovered. The detailed substrate recognition mechanisms, which are useful for drug discovery, can also be characterized. We used the Ligand of Numb protein X (LNX) family of E3s, a group of PDZ domain-containing RING-type E3 ubiquitin ligases, to demonstrate the feasibility of this strategy. Many potential substrates of LNX E3s were identified. Eight of the nine selected candidates were ubiquitinated *in vitro*, and two novel endogenous substrates, PDZ-binding kinase (PBK) and breakpoint cluster region protein (BCR), were confirmed *in vivo*. We further revealed that the LNX1-mediated ubiquitination and degradation of PBK inhibited cell proliferation and enhanced sensitivity to doxorubicin-induced apoptosis. The substrate recognition mechanism of LNX E3s was also characterized; this process involves the recognition of substrates via their specific PDZ domains by binding to the C-termini of the target proteins. This strategy can potentially be extended to a variety of E3s that contain protein interaction domain(s), thereby serving as a powerful tool for the comprehensive identification of their substrates on a proteomic scale.

**KEYWORDS:** Ubiquitination, Ubiquitin Ligase, Protein Interaction Domain, Random Peptide Library, LNX, PDZ Domain



## ■ INTRODUCTION

Ubiquitination is one of the most important protein post-translational modifications in eukaryotes.<sup>1</sup> The attachment of ubiquitin and ubiquitin-like polypeptides to intracellular proteins is a key mechanism in regulating many biological processes, including proteasome degradation, intracellular trafficking, DNA repair, and signal transduction.<sup>2</sup> The ubiquitination process is achieved through a multiple enzymatic cascade. The first step is

the attachment of free ubiquitins to a ubiquitin-activating enzyme (E1). Ubiquitin is then transferred to a ubiquitin-conjugating enzyme (E2), which along with a ubiquitin ligase (E3) ligates the ubiquitin to a specific substrate protein.<sup>3–5</sup> In this process, E3s confer specificity to the ubiquitination process

Received: March 27, 2012

Published: August 13, 2012

by recognizing target substrates.<sup>2,6–8</sup> Impaired E3s and/or their substrates can lead to a variety of human disorders such as neurodegenerative diseases and cancer.<sup>2,8</sup> The identification of this group of proteins is essential not only to reveal their functions and mechanisms but also to understand the processes in which they participate. In many instances, E3s that are involved in specific processes can be identified through functional screenings; however, most of their substrates are largely unknown.<sup>2</sup> Better, faster, and cheaper proteome-wide methods are needed to efficiently and comprehensively identify the substrates of E3s and to assign functions to known and orphan E3s.<sup>2</sup>

Recently, several powerful methods, including *in vitro* protein microarrays<sup>1,9,10</sup> and *in vivo* label-free quantitative mass spectrometry,<sup>11</sup> have been employed to identify the substrates of E3s. *In vitro* protein microarrays have been successfully used to explore the substrates of the Nedd4 family of E3s and their interaction mechanisms.<sup>1,9,10</sup> Thousands of candidate proteins were individually expressed, purified, and spotted onto arrays. Then, the candidate proteins were incubated with a reaction mixture containing the E3 of interest and FITC-labeled ubiquitin under specific conditions. This method is powerful for its high-throughput and capability of being applied to low amounts of substrates, but it is limited by the quantity and variety of candidate proteins that are covered by the arrays.<sup>1,9,10</sup> As an *in vivo* method, the label-free quantitative mass spectrometry strategy enables the identification of native substrates in physiologically relevant settings,<sup>11</sup> and it has no limitations on the quantity and variety of candidates. However, low-abundant substrates in cells are difficult to detect, due to abundance suppression during the mass spectrometry analysis.<sup>12</sup> Also, this method cannot exclude the possibility that a decrease in the levels of a candidate protein following the expression of a functional E3 is not caused by its ubiquitination.<sup>11</sup>

Numerous E3s exhibit at least one protein interaction domain or motif, such as PDZ, SH2, SH3, FHA, ankyrin repeats, and ubiquitin-like domain.<sup>13,14</sup> In most cases, E3s specifically recognize substrates via their protein interaction domains or motifs by recruiting substrates or interactors.<sup>13,14</sup> Accordingly, it is valuable to explore the substrates of E3s by screening the binding partners of their protein interaction domains. On the basis of this principle, we developed an integrated strategy to identify the substrates of E3s that contain protein interaction domains on a proteomic scale.

The Ligand of Numb protein X (LNX) family of E3s was used as an example to explain and evaluate our strategy. The human LNX family has four members,<sup>13</sup> (<http://www.hprd.org/>), and each consists of an N-terminal RING domain and several PDZ domains that are specialized for binding the extreme carboxyl termini of its target proteins.<sup>15,16</sup> Ligand of Numb protein X1 (LNX1) was originally isolated as a binding partner of the phosphotyrosine-binding domain of the cell fate determinant Numb.<sup>17</sup> It was then identified as a RING-type E3 ubiquitin ligase for the ubiquitination and degradation of Numb.<sup>18</sup> After that, one or more PDZ domains of LNX1 were reported to interact with several proteins, including CAR,<sup>19</sup> ErbB2,<sup>20</sup> SKIP,<sup>21</sup> JAM4,<sup>22</sup> CAST,<sup>23</sup> c-Src,<sup>24</sup> Claudins,<sup>25</sup> RhoC,<sup>26</sup> KCNA4,<sup>27</sup> PAK6,<sup>27</sup> PLEKHG5,<sup>27</sup> PKC- $\alpha$ 1,<sup>27</sup> TYK2,<sup>27</sup> PDZ-binding kinase (PBK),<sup>27</sup> LNX2,<sup>28</sup> and itself.<sup>28</sup> Almost all of these proteins have PDZ-binding motifs at their C-termini. A total of 107 interactors of LNX1 have been identified by several high-throughput screens using a yeast two-hybrid (Y2H) system or protein microarrays in 3 different laboratories.<sup>27,29,30</sup> Among

them, only Claudin<sup>25</sup> and c-Src<sup>24</sup> were also shown to be ubiquitination substrates of LNX1. The PDZ domains of LNX1 were further suggested to be necessary for the substrate-binding modules.<sup>25,31</sup> The other three LNX family proteins have not been studied extensively. All of the known LNX substrates had been identified individually by distinct approaches. To the best of our knowledge, no systematic work has been reported for the identification of LNX family substrates on a proteomic scale.

## ■ EXPERIMENTAL PROCEDURES

### Preparation of Plasmids and Mutagenesis

For the Y2H screenings, the bait plasmids of 11 human LNX PDZ domains were constructed; detailed clone information is summarized in Supplementary Table 1 (Supporting Information). For the *in vitro* ubiquitination assay, the full-length human LNX1, LNX1 $\Delta$ PDZ4 (1–600), LNX1 $\Delta$ PDZ34 (1–497), LNX1 $\Delta$ PDZ234 (1–377), and LNX1 $\Delta$ PDZ1234 (1–273) were amplified by PCR from IMAGE: 4995278 (Proteintech Group, Inc.) and subcloned into the BamH I/EcoR I sites of the PGEX-4T-1 vector. The individual artificial degron expressing the yeast Rpn4<sub>172–211</sub> and the C-terminal 8–10 amino acid residues of the selected candidate ligand was generated by the synthesis of oligonucleotides and ligation into the BamH I/Xho I sites of the pET 41a+ vector as previously described.<sup>32</sup> For the *in vivo* ubiquitination assay, the LNX1<sup>WT</sup> construct was made by subcloning wild-type full-length human LNX1 cDNA into the BamH I/Xba I sites of the pcDNA4/Myc-His vector (Invitrogen) and fused with a Myc tag downstream of the C-terminus of LNX1. The LNX1<sup>Mut</sup> construct, in which five conserved cysteine residues (C41, C44, C56, C61 and C64) were simultaneously mutated to alanines, was generated using PCR-directed mutagenesis. The human PBK was obtained by PCR from IMAGE: 4082846 (Proteintech Group, Inc.), constructed into the BamH I/Xho I sites of the pcDNA6/V5-His vector, and fused with the N-terminal FLAG tag. The HA-tagged ubiquitin plasmid and the His-Myc-tagged ubiquitin plasmid were kindly provided by Dr. Huihua Li (Institute of Basic Medical Sciences, Chinese Academy of Medical Sciences).

### Antibodies

All of the antibodies that were used in this study were purchased from commercial sources: anti-Myc tag (MBL, M047–3), anti-FLAG tag (DYKDDDDK) (Abmart, M20008), anti-S tag (Abcam, ab18616), anti-HA tag (Imagen BioSciences, IMA 1008 L), anti-PBK (Abcam, ab75987), anti-BCR (Abcam, ab40779), antiubiquitin (Sigma, GW10073F), anti- $\beta$ -tubulin (Abmart, M20005), anti-LNX1 (Abcam, ab76716), and anti- $\beta$ -actin (Sigma, A1978).

### Screenings

The high-diversity random peptide library used in this study, which was constructed for use in our previous work, contained  $1.5 \times 10^8$  transformed clones.<sup>32</sup> This number of clones is sufficient to cover all the possibilities of C-terminal random six amino acids ( $6.4 \times 10^7$ , 20<sup>6</sup>). Each LNX PDZ domain was used individually as bait to screen this library using the Y2H approach as previously described.<sup>32,33</sup> The specialized PDZ ligand library used in this study consisted of 424 nonredundant PDZ ligand clones, including 232 (54.72%), 81 (19.10%), 19 (4.48%), 2 (0.47%), 23 (5.42%), and 67 (15.80%) for class I, class II, class III, class IV, PDZ domain, and other ligands, respectively. A one-to-one Y2H assay was used for validation screening of this library to identify positive and negative binding clones.<sup>32</sup>

### Characterization of the Binding Properties and Identification of the Candidate Ligand Proteins

WebLogo, a sequence logo generator,<sup>34</sup> was used to analyze and graphically display the binding properties of each LNX PDZ domain that recognized the C-terminal binding motifs. Consensus binding sequences were deduced from the sequence alignment of the positive clones and from the comparative analysis of both the positive and negative sequences. The prediction and confirmation of candidate ligand proteins were performed as previously described.<sup>32</sup>

### Protein Expression and Purification

The pGEX constructs were expressed in the *E. coli* BL21 strain. The expression of the GST-fused proteins was induced with 0.1 mM IPTG at 16–25 °C overnight. The bacterial pellets were sonicated, and the GST-fused proteins in the cleared bacterial lysates were purified by GSTrap FF (GE Healthcare, 17–5130–01). The pET 41a+ constructs were expressed in the *E. coli* BL21 (DE3) strain. In this case, the expression of the His-fused proteins was induced with 0.2 mM IPTG at 30 °C for 4–6 h. The recombinant proteins were enriched by MagExtractor (His tag) (TOYOBO, NPK-701). The purified proteins were analyzed by SDS-PAGE, stained with Coomassie Blue, and quantified by the Bradford method.

### In vitro Ubiquitination Assay

The *in vitro* ubiquitination assays were performed using 0.1 µg E1 (Calbiochem, 662070), 0.5 µg E2 (UbcH5b, recombinant) (UpState, 14–871), 1 µg E3 (LNX truncations), 2 mM ATP, 3 µg ubiquitin (Sigma-Aldrich, U5507), 50 mM Tris-HCl (pH 7.4), 2.5 mM MgCl<sub>2</sub>, 1 mM DTT, and 50–100 ng substrates. The mixture was incubated at 30 °C for 90 min, and the reaction was stopped by adding 5 × SDS loading buffer (GenStar Biosolutions, E153–01). The reaction mixture was resolved by SDS-PAGE and immunoblotted with an anti-S tag antibody.

### In vivo Ubiquitination and Degradation Assays

HEK293ET cells and HeLa cells were used for the *in vivo* assays. They were cultured under conventional conditions (<http://www.atcc.org/>). The plasmid transfection was performed with the MegaTran 1.0 Transfection Reagent (OriGene, TT200003). The harvested cells were lysed with RIPA lysis buffer (Applygen, P1053) containing 2 mM PMSF, and the cleared cell lysates were incubated with appropriate antibodies at 4 °C overnight. The immunocomplexes were bound to protein G agarose beads (Beyotime, P2009) for 1–3 h, washed three times with cold PBS buffer, and eluted by boiling in 5× SDS loading buffer. The proteins were separated by SDS-PAGE and immunoblotted with appropriate antibodies. For the detection of protein degradation, the cleared cell lysates were directly separated by SDS-PAGE and immunoblotted with appropriate antibodies. In an experiment that used a proteasome inhibitor, the transfected cells were incubated with 10–20 µM MG132 (Beyotime, S1748) for 10–24 h before they were harvested.

### RNAi Assay

The siRNAs, including siLNX1 (Trilencer-27, OriGene, SR313643) and siNEG.2 (negative control, Trilencer-27, OriGene, SR30004), were purchased from OriGene (Rockville, MD). The siRNA was transfected using siTran 1.0 transfection reagent (OriGene, TT300001). Three days after transfection, the cells were harvested and lysed with RIPA lysis buffer (Applygen, P1053) containing 2 mM PMSF. The cleared cell lysates were separated by SDS-PAGE and immunoblotted with appropriate antibodies.

### Cell Growth Studies

The MTS (3-(4,5-dimethylthiazol-2-yl)-5-(3-carboxymethoxyphenyl)-2-(4-sulfophenyl)-2H-tetrazolium, inner salt) cell proliferation assay was used to analyze the proliferation of MCF-7 cells following the manufacturer's instructions (Promega, USA). MCF-7 cells and HEK293T cells were cultured under conventional conditions (<http://www.atcc.org/>). LNX1<sup>WT</sup>-pcDNA4 and pcDNA4 (vector control) were transfected into MCF-7 cells with poly-Factor II (Beijing ViewSolid Biotechnology Co., Ltd., VS1001B), respectively. Twelve hours after transfection, 200 µg/mL Zeocin (Invitrogen) was added to the cell culture medium to select the transfected cells. Twenty-four hours after transfection, the 96-well microtiter plates were seeded with 1 × 10<sup>4</sup> cells per well. A total of 40 µL MTS was added to 200 µL of the cell culture medium, and the mixtures were incubated at 37 °C for 1 h prior to measurement. The absorbances of the transfected cells and the control DMEM medium at 492 nm were measured using Synergy4 Multi-Mode Microplate Readers (BioTek, USA) at 0, 12, 24, 36 and 60 h. For RNAi assay, the siLNX1 and siNEG.2 (negative control) were transfected into HEK293T cells, respectively. Twenty-four hours after transfection, the 96-well microtiter plates were seeded with 5 × 10<sup>3</sup> cells per well. Cell growth was monitored using the MTS method at 0, 12, 24, 36 and 48 h. The data were analyzed by one-way ANOVA analysis with SPSS 13.0. The averaged results were presented as the mean value ± SEM of the indicated experiments. Statistical significance was evaluated using Student's *t*-test. Asterisks were used to denote statistical significance compared to the control, indicating *p*-values of less than 0.05 (\*), 0.01 (\*\*), and 0.001 (\*\*\*).

### Gene Ontology (GO) Term Enrichment Analysis

The PANTHER (Protein ANALysis THrough Evolutionary Relationships) classification system<sup>35</sup> was used for GO category enrichment analysis. The LNX1 ligand genes were classified into three functional categories: molecular function, biological process, and protein class. The enrichments or overrepresentations of these categories for the LNX1 ligand genes were compared to their representation in the entire human genome. Genes for which no annotations could be assigned were excluded from the analysis for both the ligands and the genome set. Categories with at least three genes were displayed in the bar charts.

## RESULTS

### 1. Proteomics Strategy to Identify Substrates of LNX Family of E3s

The newly developed strategy involved the following steps, as illustrated in Figure 1. **Step 1: Screening random peptide libraries with LNX PDZ domains.** Individual screenings of random peptide libraries and/or validation screenings of a specialized PDZ ligand library, using each LNX PDZ domain as bait, were performed to isolate a series of positive PDZ-binding clones. **Step 2: Characterizing the binding properties and identifying candidate ligand proteins.** The precise binding properties of each PDZ were characterized by comparative analysis of both positive and negative binding sequences that were isolated from the screenings. The ligand proteins were predicted by protein database searches with consensus binding sequences. The candidate ligands were further confirmed by one-to-one Y2H assays. **Step 3: Validating the effect of the C-terminal PDZ-binding motif of candidate ligands using an *in vitro* ubiquitination assay.** Artificial degron proteins, used as

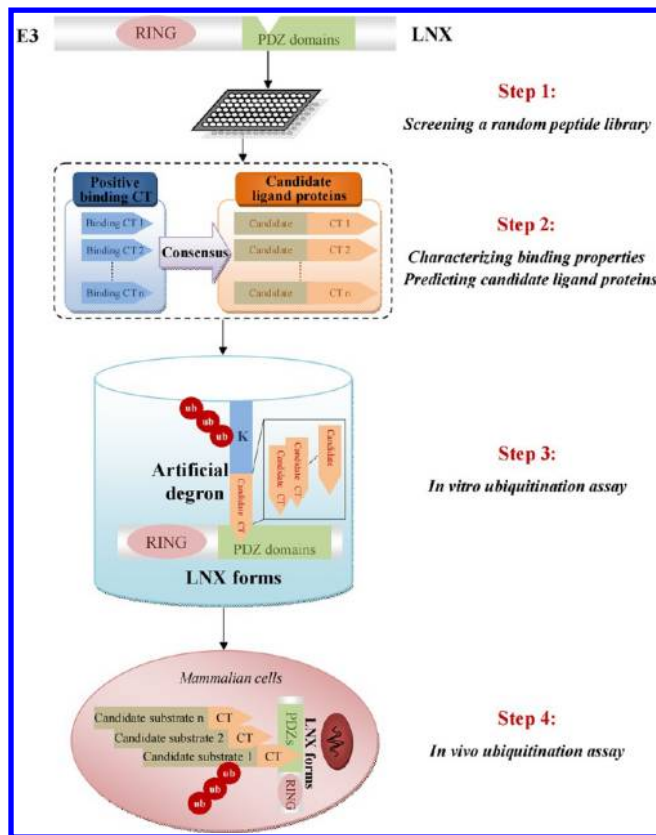


**Figure 1.** Schematic of the newly developed proteomics strategy to identify substrates of E3s containing protein interaction domains. LNX E3 was used as an example to illustrate our strategy. The detailed description was presented in the part 1 of the Results section. CT denotes the C-terminus of a protein.

potential substrates, expressing a preferential ubiquitination sequence (Rpn4<sup>172–211</sup>, including one lysine residue)<sup>36</sup> and the C-terminal PDZ-binding motifs of candidate ligand proteins, were individually constructed, expressed, and purified. The respective LNX protein forms, expressing the RING domain and the corresponding PDZ domains, were also prepared. The *in vitro* ubiquitination assays were individually conducted with the respective artificial degrons and the LNX forms to confirm whether the C-terminal PDZ-binding motif of the candidate

ligands could promote ubiquitination. **Step 4: Confirming the LNX substrates in mammalian cells using an *in vivo* ubiquitination assay.** Candidate substrates and LNX E3 were cotransfected into mammalian cells to confirm whether LNX could induce the ubiquitination and degradation of the candidate substrates.

In step 1 of this strategy, any screening methods for characterizing the binding properties of the protein interaction domains can be adopted, including oriented peptide library,<sup>15,37,38</sup> SPOT synthesis,<sup>39</sup> phage display,<sup>40</sup> and conventional Y2H.<sup>41</sup> Additionally, both the native ligand proteins that were retrieved from the screenings in step 1 and the candidate ligand proteins that were identified in step 2 can be directly confirmed in mammalian cells, thus bypassing step 3.

## 2. Characterization of the Binding Properties of the LNX PDZ Domains

We employed our previously developed validation screening strategy<sup>32</sup> for the comprehensive analysis of PDZ domains in the LNX family. The binding properties of all 11 LNX PDZs were individually characterized by Y2H screenings of random peptide libraries and/or high-throughput validation screenings of the specialized PDZ ligand library. LNX1 PDZ1, LNX1 PDZ2, LNX1 PDZ3, LNX2 PDZ2, and LNX4 PDZ showed strong consensus binding properties located at the C-terminal 3 to 5 amino acid residues of positive binding ligands that were isolated from the screenings (Supplementary Table 2–6, Supporting Information). LNX2 PDZ1 and LNX2 PDZ3 showed no consensus among the positive binding sequences (Supplementary Tables 7 and 8, Supporting Information). LNX1 PDZ4 and LNX2 PDZ4 retrieved no positive binding ligands from screenings of either random peptide libraries or the PDZ ligand library. LNX3 PDZ1 and PDZ2 exhibited variable levels of self-activation in the Y2H system and thus could not be used to screen the libraries.

The detailed binding specificities of each LNX PDZ domain are summarized in Table 1 and illustrated in Figure 2. PDZ-binding motifs have conventionally been grouped into four classes, based on the last four residues: Class I,  $-[S/T]-x-\Phi^*$ ; Class II,  $-\Phi-x-\Phi^*$ ; Class III,  $-[D/E/K/R]-x-\Phi^*$  and Class IV,  $-x-\psi-[D/E]^*$ , where  $x$  is any amino acid,  $\Phi$  is a hydrophobic residue, and  $\psi$  is an aromatic residue.<sup>42</sup> LNX1 PDZ1 predominantly preferred Ser and Thr at P<sup>2-</sup> (−2 position of PDZ-binding motif), and thus belonged to the typical Class I PDZ. LNX1

**Table 1.** Binding Properties of Human LNX PDZ Domains<sup>a</sup>

LNX PDZ domain	amino acid preference at each position of C termini of PDZ binding ligands						PDZ domain type	characterization methods
	−5	−4	−3	−2	−1	0		
LNX1	PDZ1	x	x	x	S/T	x	V/I/L/C	Validation screening of PDZ ligand library
	PDZ2	x	x	x	x	$\psi$	V/I/L/C	
	PDZ3	x	$\psi$	x	x	$x-\psi$	V/I/L/C	
	PDZ4				N/A		PDZ	
LNX2	PDZ1				No consensus at the C termini		PDZ	Screening of random peptide library and Validation screening of PDZ ligand library
	PDZ2	x	x	$\Phi$	V/I/L/S/T	V/I/L	V/I/L	
	PDZ3				No consensus at the C termini		Atypical	
	PDZ4				N/A		PDZ	
LNX3	PDZ1				Bait self-activation		N/A	N/A
	PDZ2				Bait self-activation		N/A	
LNX4	PDZ	$\psi$	x	$\psi/x$	F/x	K/R/H	V/I/L	II

<sup>a</sup> $x$  denotes any amino acid;  $\Phi$  denotes hydrophobic amino acids;  $\psi$  denotes aromatic amino acids;  $x-\psi$  denotes any amino acid excluding aromatic amino acids;  $\psi/x$  denotes any amino acid can be recognized while  $\psi$  is preferred, the same as others; N/A denotes not available.

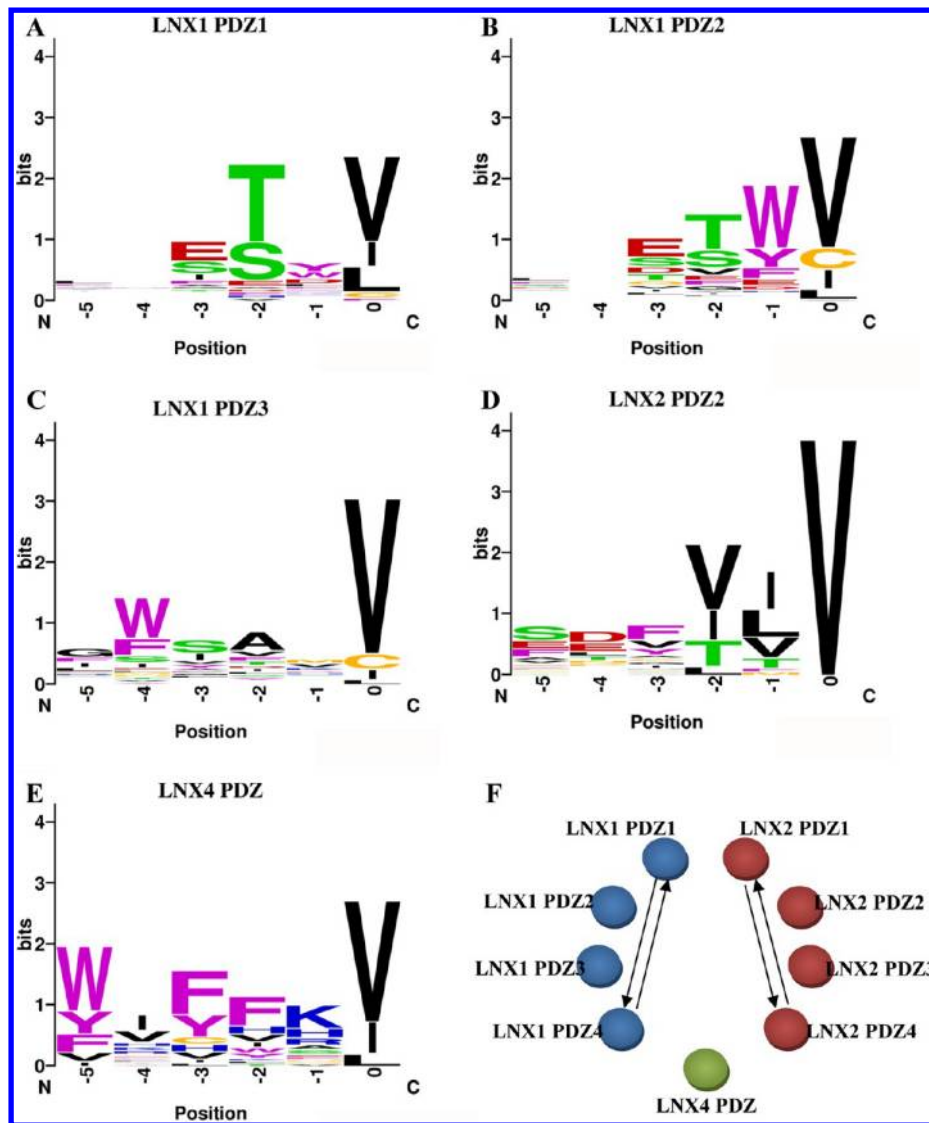


**Figure 2.** Binding properties of LNX PDZ domains. (A) LNX1 PDZ1, (B) LNX1 PDZ2, (C) LNX1 PDZ3, (D) LNX2 PDZ2, and (E) LNX4 PDZ showed strong consensus binding properties at the C-termini of the respective positive binding sequences isolated from Y2H screenings of random peptide libraries and/or validation screenings. The preference of each amino acid at each position was graphically displayed as logos. The positions were numbered from the carboxyl terminus (position 0). (F) PDZ-PDZ interactions of the LNX family. Two pairs of the PDZ-PDZ interactions were discovered and confirmed, namely LNX1 PDZ1 and LNX1 PDZ4 and LNX2 PDZ1 and LNX2 PDZ4. Both of these two interactions were determined in both the forward Y2H assay (BD→AD, e.g., the bait BD-LNX1 PDZ1 bound to the prey AD-LNX1 PDZ4) and the reverse Y2H assay (AD→BD, e.g., the prey AD-LNX1 PDZ1 bound to the bait BD-LNX1 PDZ4), as shown by the arrows.

PDZ2 showed no selectivity at P<sup>2-</sup> but preferred  $\psi$  at P<sup>1-</sup>. LNX1 PDZ3 did not select  $\psi$  at P<sup>1-</sup> (derived from negative binding sequences), but it preferred  $\psi$  at P<sup>4-</sup>. LNX2 PDZ2 recognized both Class I and II binding motifs and showed a slight preference for  $\Phi$  at P<sup>3-</sup>. LNX4 exhibited a predominant preference of basic amino acids at P<sup>1-</sup> and strongly preferred  $\psi$  at P<sup>5-</sup>. All of these five PDZs recognized more than one conventional class of ligands as well as unclassified PDZ ligands. As increasing novel types of PDZ-ligand interactions being reported,<sup>32,43-45</sup> the traditional classification system is no longer capable of differentiating all of the PDZ domains, and it needs to be revised.

Because the clones of PDZ domains were included in the specialized PDZ ligand library,<sup>32</sup> we also systematically characterized the PDZ-PDZ interactions of the LNX family. Three pairs of PDZ-PDZ interactions were discovered, namely LNX1 PDZ1 and LNX1 PDZ4, LNX1 PDZ1 and LNX2 PDZ4, and LNX2 PDZ1 and LNX2 PDZ4. All of these interactions were

determined in both the forward (BD→AD) and reverse (AD→BD) Y2H assays. The LNX1/LNX2 PDZ4 constructs used in our Y2H assays included the natural carboxy-terminal PDZ motifs. For clarifying the three interactions, including LNX1 PDZ1 and LNX1 PDZ4, LNX1 PDZ1 and LNX2 PDZ4, and LNX2 PDZ1 and LNX2 PDZ4 were whether PDZ:PDZ interaction or PDZ:C-terminal binding motif interaction, we tested the interaction between LNX1/LNX2 PDZ1 and the C-termini of LNX1/LNX2 in one-to-one Y2H assays, respectively. The clones expressing the C-terminal 10 amino acids of LNX1/LNX2 were individually constructed by the synthesis of oligonucleotides and were cotransformed into yeast cells with LNX1/LNX2 PDZ1 bait, respectively. The results showed that LNX1 PDZ1-LNX1 PDZ4 interaction and LNX2 PDZ1-LNX2 PDZ4 interaction were true PDZ:PDZ interactions because neither LNX1 PDZ1 nor LNX2 PDZ1 interacted with their own C-termini (Figure 2F). Interaction between LNX1 PDZ1 and C-termini of LNX2

Table 2. Identified LNX Ligand Proteins<sup>42</sup>

LNX	binding PDZ	consensus sequence	identified LNX1 ligands		
			Swiss-Prot ID	C-terminus	protein description
LNX1	PDZ1	-[S/T]-ψ-V*	Q7Z5N4-1	LTGFSSFV	Isoform 1 of Protein sidekick-1 precursor
			Q1MX18-1	SNMEESFV	Isoform 1 of Protein inscuteable homologue
			Q92823-1	VNAMNSFV	Splice isoform 1 OF Neuronal cell adhesion molecule precursor
			Q5VX33	EKVKEYV	ATP-binding cassette, subfamily A member 1
			O60229	GDPFSTYV	Huntingtin-associated protein-interacting protein (Duo protein)
			P56750	SKTSTSYV	Claudin-17
			Q8NGB0	MDGNSSWV	Seven transmembrane helix receptor
			Q8IYI6	PESTTSV	Exocyst complex component 8
			Q9BZ29-4	MTSSSVV	Isoform 4 of Dedicator of cytokinesis protein 9
			Q96PB8	PDDISTV	Leucine-rich repeat-containing protein 3B precursor
			Q5V5F5	DPSVSTV	Glutamate receptor, ionotropic, N-methyl D-aspartate 1
		-[S/T]-L-V*	O43182-1	DALPETLV	Isoform 3 of Rho-GTPase-activating protein 6
			<b>Q8N448</b>	<b>ICWPGSLV</b>	<b>Ligand of Numb protein X 2</b>
			P32745	STMRIYS	Somatostatin receptor type 3 (SS3R) (SSR-28)
			P25100	SNLRETDI	Alpha-1D adrenergic receptor
			Q9H2J7	PDMPESDL	Orphan transporter v7-3
			<b>Q96KB5</b>	<b>VEALETDV</b>	<b>spermatogenesis-related protein kinase (PDZ-binding kinase)</b>
			Q9HBX8	GLAFASHV	Leucine-rich repeat-containing G protein-coupled receptor 6
			Q06418	GLLPHSSC	Tyrosine-protein kinase receptor TYRO3
			Q99966	TADFPSSC	Cbp/p300-interacting transactivator 1
			Q9P2M7	SNLQTSSC	Cingulin
	PDZ2	-A-[S/T]-[K/R/H]-V*	P43119	ASVACSLC	Prostacyclin receptor
			Q9Y345	DLELGTQC	Sodium- and chloride-dependent glycine transporter 2
			P57058	ADGVKTQC	Hormonally upregulated neu tumor-associated kinase
			P48546	SRELESYC	Gastric inhibitory polypeptide receptor
			O00192	PQPVDSWV	ARVCF
			Q9UQB3	PASPDWV	Catenin delta-2
			Q99569-2	PGSPDSWV	p0071(plakophilin-4)
			P56750	SKTSTSYV	Claudin-17
			O60229	GDPFSTYV	Huntingtin-associated protein-interacting protein
			Q8NHY3	PPEEESWV	GAS2-related protein isoform beta
		-[S/T/D/E]-ψ-V*	<b>O95832</b>	<b>PSSGKDYV</b>	<b>Claudin-1</b>
			P49815	VEDFTEFV	Tuberin
			Q8N2R7	RARKSEWV	Connexin40.1
			Q9Y5U5	GRLGDLWV	Tumor necrosis factor receptor superfamily member 18
			<b>P57739</b>	<b>SYSLTGYV</b>	<b>Claudin-2</b>
			Q12906-5	TAGYTGfV	Interleukin enhancer binding factor 3 isoform c
	-[V/F]-[F/Y]-[V/I/L]*	P43234	DSVSSIFV	Cathepsin O	
		Q86Y07	VFLALFFL	Serine/threonine-protein kinase VRK2	
		Q9H1J5	RVWFGVYI	Wnt-8a protein	
		O43815	DALAKVfV	Striatin	
		<b>P15385</b>	<b>AKAVETDV</b>	<b>Potassium channel Kv1.4</b>	
		Q99434	RLRVETDV	ARHGEF16 protein	
		P03409	KHFRETEV	TAX_HTLV-1	
	PDZ3	-[P/L]-[G/S]-W-S-A-[M/V]-V*	O60828-9	CPGWSAMV	Isoform 9 of Polyglutamine-binding protein 1
			Q9H3Q1	EEDEIRV	Cdc42 effector protein 4
			Q9P0R7	LKIFLSKV	HSPC209
Q9NP55			GLQFVIK	Protein Plunc precursor	
Q304Z4			DRFKAHV	Envelope polyprotein	
-[W/F]-x-x-[D/E]-V*		Q12979	TLYFSTDV	Isoform Long of ABR protein	
		Q15040	HQSWRTDV	Josephin-1	
		Q8NfH4	LLFWVTEV	Nucleoporin Nup37	
		P11274	SILFSTEV	Breakpoint cluster region protein	
		Q9BZT2	DTAWSREV	PNAS-32	
		P41595	TEEQVSYV	5-hydroxytryptamine 2B receptor	
		-V-S-Y-V*	<b>P78310-2</b>	<b>KTDGITV</b>	<b>Isoform 2 of CAR precursor</b>
			Q9NTG1	KKMVYLV	PKD and REJ homologue
LNX2	PDZ2	-Φ-[V/I/L/T]-[V/I/L/T]-V*	Q9UPQ7	SFLSVTTV	LNX 3
			Q6ZMN7	AFLSVTTV	LNX 4

Table 2. continued

LNKX	binding PDZ	consensus sequence	identified LNX1 ligands		
			Swiss-Prot ID	C-terminus	protein description
			Q5T3H7	ESGICTIV	similar to TPR repeat-containing protein KIAA1043
			Q8NFP4-2	GNHVALTV	MAM domain-containing protein 3
			O00257-1	TFKEYVTV	chromobox homologue 4
			Q6UWI4	KMYPVTV	Transmembrane protein 46 precursor
LNKX4	PDZ	$-\psi-x-x-x-[K/R/H]-V^*$	Q6ZW25	NKYKLYKV	CDNA FLJ41726 fis, clone HLUNG2014449

<sup>a</sup>Bold text denotes known ligand proteins, x denotes any amino acid,  $\Phi$  denotes hydrophobic amino acids, and  $\psi$  denotes aromatic amino acids.

was detected (data not shown), indicating that LNX1 PDZ1 could recognize LNX2 via the C-terminal PDZ motif.

### 3. Identification of Candidate LNX Ligand Proteins

For each of the five PDZ domains that recognized the C-terminal binding motifs, the consensus binding sequences (Table 2) were deduced from the sequence alignment of positive clones and/or the comparative analysis of positive and negative binding sequences. The Tailfit software<sup>46</sup> was used to search the Swiss-Prot and/or IPI human databases to retrieve potential ligand proteins whose C-termini matched the consensus binding sequences. The candidate ligand proteins (Supplementary Tables 9–13, Supporting Information) were further selected based on their subcellular localizations and molecular functions. The selected ligand proteins were confirmed in subsequent one-to-one Y2H assays. The clones expressing the C-termini of the selected PDZ ligands were individually constructed by the synthesis of oligonucleotides and were cotransformed into yeast cells with the corresponding PDZ bait.

As shown in Table 2, 64 ligands were confirmed, and of these, 6 ligand proteins had been previously determined to be the physiological substrates or interactors of LNX by other independent laboratories. Claudin-1 and Claudin-2 had been demonstrated to be polyubiquitinated by LNX1 in mammalian cells, followed by endocytosis and degradation in lysosomes, and their ubiquitination regulated the turnover of tight junctions.<sup>25</sup> LNX2 had been shown to interact with LNX1 to form oligomers via their PDZ domain-recognizing PDZ-binding motifs located at the C-termini; therefore, LNX proteins may form large networks that serve as molecular scaffolds to localize unrelated, interacting proteins, such as Numb, to specific subcellular sites in cells.<sup>28</sup> CAR-2 had been shown to bind LNX2 both *in vitro* and *in vivo*, and also colocalize with LNX2 in mammalian cells.<sup>19,47</sup> PBK and Potassium channel Kv1.4 (KCN4) had been demonstrated to coimmunoprecipitate with LNX1.<sup>27</sup>

### 4. LNX Substrate Recognition Requires the C-Terminal PDZ-Binding Motif of the Ligand Proteins

The substrate proteins that are specifically recognized by E3 ubiquitin ligases require a ubiquitination signal (degron), which is a minimal element within a protein that is sufficient for the recognition and ubiquitination by the proteolytic apparatus.<sup>48</sup> A degron is composed of a ubiquitination acceptor site and a ubiquitination signal.<sup>48</sup> We hypothesized that the C-terminal PDZ-binding motif of ligand proteins might function as the ubiquitination signal that is recognized by the corresponding LNX PDZs to promote the subsequent ubiquitination.

To test this idea, we designed an *in vitro* ubiquitination system. We first constructed and purified artificial degron proteins to serve as potential substrates. They consisted of an ubiquitination site sequence, Rpn4<sub>172–211</sub> (residues 172–211 of Rpn4 protein),<sup>36</sup> and different C-termini of LNX ligand proteins, as

depicted in Figure 3A. Rpn4<sub>172–211</sub> possesses one lysine (K) amino acid residue that is a preferential ubiquitination site

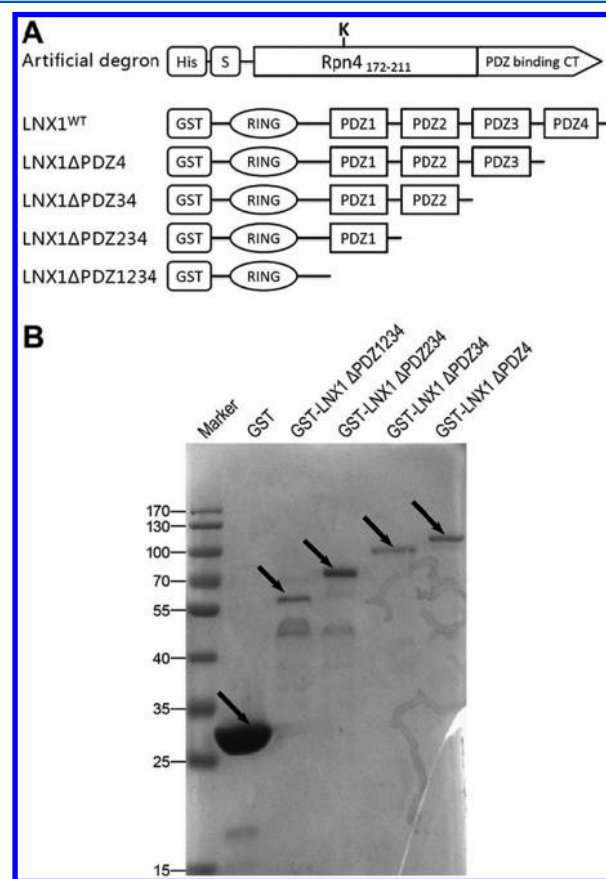


**Figure 3.** (A) Schematic representation of the artificial degrons and LNX1 truncations. An artificial degron consisted of an N-terminal a tandem His and S tag for purification and detection, Rpn4<sub>172–211</sub> (which possesses one lysine (K) amino acid residue as a ubiquitination acceptor site), and the C-terminal PDZ binding motif of the LNX ligand protein. The LNX1 truncations consisted of an N-terminal GST tag for purification, a RING domain, and of either no, one or more PDZ domains. (B) Purification of the LNX1 truncations for the *in vitro* ubiquitination assays. GST-LNX1 truncation proteins were expressed in the *E. coli* BL21 strain and purified by GSTrap FF.

selected from a group of lysines susceptible for ubiquitination in the substrate.<sup>36</sup> Nine C-terminal PDZ-binding motifs of the LNX1 ligand proteins were selected and individually constructed to the C-terminus of Rpn4<sub>172–211</sub>. The non-PDZ-binding vector sequence -PPPPPLID\* was used as a negative control. Each artificial degron was fused with a tandem His and S tag at the N-terminus for purification and detection. A series of GST-tagged LNX1 truncations (depicted in Figure 3A) were constructed and

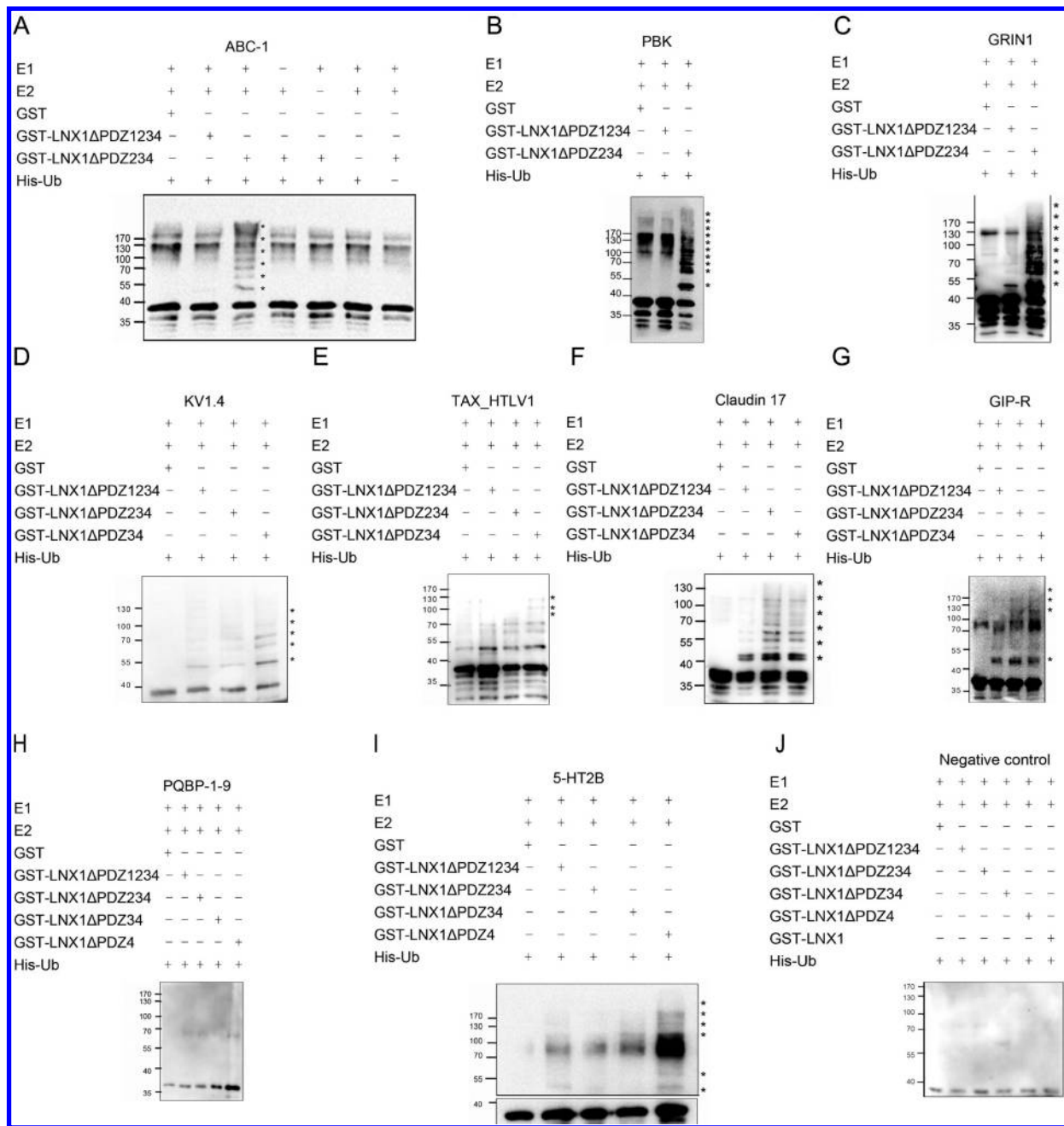


**Figure 4.** Validating the effect of the C-terminal PDZ-binding motifs of candidate ligands by the *in vitro* ubiquitination assay. Nine His/S-tagged artificial degress terminated with the C-termini of the nine selected LNX1 ligand proteins, GST-LNX1 E3 forms, E1, E2 (UbcH5b), and ubiquitin were incubated with the ubiquitination reaction buffer at 30 °C for 90 min. They were then separated by SDS-PAGE and immunoblotted with an anti-S tag antibody. In the first row, three artificial degress were terminated with the C-termini of LNX1 PDZ1 ligand proteins. In the second row, three artificial degress were terminated with the C-termini of LNX1 PDZ2 ligand proteins and Claudin 17 artificial degress were terminated with both the C-termini of LNX1 PDZ2 and LNX1 PDZ1 ligand proteins. In the third row, three artificial degress were terminated with the C-termini of LNX1 PDZ3 ligand proteins and the non-PDZ-binding vector sequence -PPPPPLID\*. Eight of the nine artificial degress, all except the PQBP-1–9 artificial degress, were ubiquitinated by the corresponding LNX1 E3 forms.

purified to act as E3 ligases (Figure 3B). To determine whether the C-terminal PDZ-binding motif could promote ubiquitination, the artificial degress and the corresponding GST-LNX1 E3 form were added into the *in vitro* ubiquitination reaction and incubated with ubiquitin, E1, and E2 (UbcH5B). The ubiquitination of the artificial degress was measured by detection with an anti-S tag antibody.

As shown in Figure 4, eight of the nine artificial degress were ubiquitinated by the corresponding LNX1 E3 forms, as

summarized in Table 3. The C-terminal LNX1 PDZ1-binding motifs of the ATP-binding cassette, subfamily A member 1 (ABC-1), PBK, glutamate receptor, ionotropic, *N*-methyl *D*-aspartate 1 (GRIN1), and Claudin-17 significantly promoted the ubiquitination of the corresponding artificial degress by LNX1ΔPDZ234. The C-terminal LNX1 PDZ2-binding motifs of the potassium channel Kv1.4, TAX\_HTLV-1, Claudin-17, and gastric inhibitory polypeptide receptor (GIP-R) promoted ubiquitination by LNX1ΔPDZ34; however, these four artificial

Table 3. Results of *in vitro* Ubiquitination Assay

LNX1 forms	C termini of artificial degrons			ubiquitination results
	candidate substrates	sequence	binding PDZ	
LNX1 $\Delta$ PDZ234	ATP-binding cassette, subfamily A member 1 (ABC-1)	EKVKEYSYV*	LNX1 PDZ1	+
	PDZ-binding kinase (PBK)	VEALETDV*		+
	Glutamate receptor, ionotropic, N-methyl D-aspartate 1 (GRIN1)	DPSVSTVV*		+
	Claudin-17	SKTSTSYV*		+
LNX1 $\Delta$ PDZ34	Potassium channel Kv1.4 (Kv1.4)	AKAVETDV*	LNX1 PDZ2	+
	TAX_HTLV1	KHFRETEV*		+
	Claudin-17	SKTSTSYV*		+
	Gastric inhibitory polypeptide receptor (GIP-R)	SRELESYC*		+
LNX1 $\Delta$ PDZ4	5-hydroxytryptamine 2B receptor (5-HT2B)	TEEQVSYV*	LNX1 PDZ3	+
	Isoform 9 of Polyglutamine-binding protein 1 (PQBP-1-9)	CPGWSAMV*		-

degrons showed various degrees of cross-ubiquitination with LNX1 $\Delta$ PDZ234. This could have resulted from the similar binding properties of PDZ1 and PDZ2, so that the C-termini of these four proteins could also be recognized by LNX1 PDZ1 in different degree. The C-terminal LNX1 PDZ3-binding motifs of the 5-hydroxytryptamine 2B receptor (5-HT2B) promoted ubiquitination by LNX1 $\Delta$ PDZ4. However, the ubiquitination of the artificial degron that was terminated with isoform 9 of polyglutamine-binding protein 1 (PQBP-1-9) was not detected. The artificial degron that was used as a negative control was not ubiquitinated by any of the LNX1 E3 forms. Therefore, our *in vitro* ubiquitination results indicated that these eight ligand proteins were potentially physiological substrates of LNX1 *in vivo*.

### 5. Confirmation of the Substrates of LNX1 in Mammalian Cells

Because artificial degrons have only C-terminal PDZ-binding motifs of the ligand proteins, they may not accurately reflect the behavior of native full-length proteins. Endogenous proteins were further validated to determine whether they were the actual substrates of LNX1 E3 in mammalian cells.

First, PBK and breakpoint cluster region protein (BCR) were tested by *in vivo* ubiquitination assays. Myc-tagged LNX1<sup>WT</sup> and LNX1<sup>Mut</sup> were transfected into HEK293ET cells with HA-tagged ubiquitin, respectively. LNX1<sup>Mut</sup> is the LNX1 RING domain mutant form, within which five of seven key Cys residues of the RING domain<sup>2</sup> are mutated to Ala residues and which is supposed to abolish the LNX1 E3 ligase activity. The endogenous PBK or BCR were immunoprecipitated from cell lysates with the corresponding antibodies and immunoblotted with the anti-HA or anti-ubiquitin antibodies to detect their ubiquitination. As shown in Figure 5A and B, in the presence of LNX1<sup>WT</sup>, both PBK and BCR were significantly modified by ubiquitin as indicated by the high-molecular-weight discrete bands and smear, whereas very faint ubiquitination bands were observed when LNX1<sup>Mut</sup> was expressed. The results distinctly indicate that LNX1 promoted the ubiquitination of endogenous PBK and BCR in mammalian cells.

The ubiquitination of cellular proteins often leads to their degradation by the proteasome.<sup>18</sup> Next, we estimated whether LNX1-induced ubiquitination of PBK and BCR causes their degradation. The effect of LNX1 on overexpressed recombinant PBK was first assessed. As shown in Supplementary Figure 1 (Supporting Information), the dramatic degradation of FLAG-tagged PBK was observed in the presence of LNX1<sup>WT</sup>, whereas only partial degradation was observed with LNX1<sup>Mut</sup>. Endogenous PBK and BCR were further assessed in mammalian cells.

LNX1<sup>WT</sup> and LNX1<sup>Mut</sup> were transfected into HeLa cells, respectively. Cell lysates were separated and immunoblotted using anti-PBK or anti-BCR antibodies. As shown in Figure 5C and D, both endogenous PBK and BCR were significantly degraded in the presence of LNX1<sup>WT</sup>, whereas only partial degradation was observed with LNX1<sup>Mut</sup>. When transfected cells were treated overnight with MG132, the degradations were remarkably blocked. To quantify the degradation of endogenous PBK and BCR induced by LNX1<sup>WT</sup>, we performed the experiments in triplicate followed by densitometry of the immunoreactive bands. As shown in Figure 5E, 50% reduction of PBK was observed in the presence of LNX1<sup>WT</sup>, and MG132 partially blocked the decrease (the raw data was shown in Supplementary Table 14). Further validation (shown in Supplementary Figure 2) indicated that PBK was not degraded via the lysosome pathway. The fact that MG132 only partially blocks the degradation of PBK implied that PBK may be degraded also via other unknown ways. As shown in Figure 5F, approximately 40% reduction of BCR was observed, and MG132 significantly blocked the decrease to the basal level (the raw data was shown in Supplementary Table 15). These results indicated that LNX1 promoted the degradation of PBK and BCR mainly in a proteasome-dependent manner.

### 6. Physiological Significance of the PBK-LNX1 E3 Partnership

PBK is a serine/threonine kinase<sup>49</sup> and contributes to tumor development and growth.<sup>50-53</sup> Park et al. and Ayllon et al. demonstrated that the siRNA-mediated reduction of PBK expression suppressed breast cancer cell growth.<sup>50,51</sup> Hu et al. reported that stable PBK knockdown cell lines (derived from MCF-7 cells) showed increased apoptosis and slower growth, and they suggested that PBK overexpression might promote tumor cell survival and resistance to chemotherapy-induced apoptosis.<sup>54</sup> To confirm that PBK is in fact the physiological substrate of LNX1 E3 under normal circumstances, we used LNX1-specific siRNA (siLNK1) to reduce its expression and assessed the expression of PBK. As shown in Figure 6A, 85% knockdown of endogenous LNX1 was detected in HEK293T cells by siLNK1, while the expression of endogenous PBK was elevated significantly ( $p < 0.05$  for 3 independent experiments). (all the raw data were quantified using ImageJ and were shown in Supplementary Table 16, Supporting Information). The endogenous LNX1 band detected by anti-LNX1 antibody had the same molecular weight as Myc-LNX1 p80 detected by anti-Myc antibody (shown in Supplementary Figure 3). The result indicated that the endogenous LNX1 expressed in HEK cells is the p80 form.

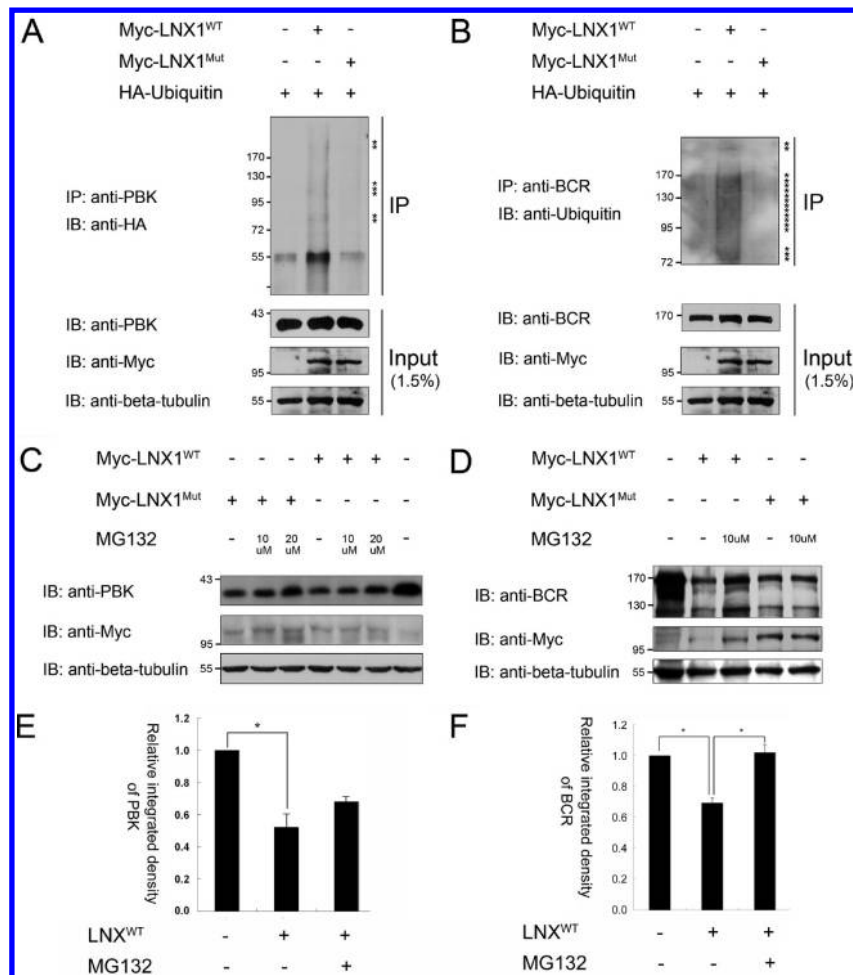


**Figure 5.** Confirmation of the LNX1 substrates in mammalian cells by the *in vivo* ubiquitination and degradation assay. (A) Myc-tagged LNX1<sup>WT</sup> and LNX1<sup>Mut</sup> were transfected into HEK293ET cells with HA-tagged ubiquitin respectively. The endogenous PBK was immunoprecipitated from the cell lysates with the anti-PBK antibody and immunoblotted with the anti-HA antibody to detect its ubiquitination. The significant ubiquitination bands of PBK were observed in the LNX1<sup>WT</sup> lane, whereas only very faint ubiquitination bands were observed in the LNX1<sup>Mut</sup> lane. (B) Myc-tagged LNX1<sup>WT</sup> and LNX1<sup>Mut</sup> were transfected into HEK293ET cells with HA-tagged ubiquitin respectively. Endogenous BCR was immunoprecipitated with the anti-BCR antibody and immunoblotted with the anti-ubiquitin antibody. The endogenous BCR was ubiquitinated when LNX1<sup>WT</sup> was expressed, whereas only partial ubiquitination bands were observed when LNX1<sup>Mut</sup> was expressed. (C) Myc-tagged LNX1<sup>WT</sup> and LNX1<sup>Mut</sup> were transfected into HeLa cells, respectively. Protein lysates of the transfected cells were separated by SDS-PAGE and immunoblotted with the anti-PBK antibody. The expression of LNX1<sup>WT</sup> induced the significant degradation of endogenous PBK, whereas only partial degradation was observed with LNX1<sup>Mut</sup>. When transfected cells were treated overnight with 10  $\mu$ M or 20  $\mu$ M MG132, the degradation of PBK was remarkably blocked. (D) HeLa cells were transfected with Myc-tagged LNX1<sup>WT</sup> and LNX1<sup>Mut</sup>, respectively. The transfected cell lysates were separated by SDS-PAGE and immunoblotted with the anti-BCR antibody. Two bands of endogenous BCR with molecular weights of 170 kDa and 120 kDa were detected. Both BCR bands were significantly decreased when LNX1<sup>WT</sup> was expressed, whereas only partial degradation was observed with LNX1<sup>Mut</sup>. When transfected cells were incubated overnight with 10  $\mu$ M MG132, the degradation of endogenous BCR was remarkably blocked. To calculate the relative extent of endogenous PBK and BCR, the signal of (E) PBK and (F) BCR was quantified using ImageJ software, divided by the corresponding loading control signal and normalized to 1.0. The averages and S.E.M.s from three independent experiments are shown.

To study the physiological significance of LNX1-mediated ubiquitination and degradation of PBK, we studied the phenotypic changes regarding proliferation and sensitivity to apoptosis in LNX1 overexpressed or knockdown cells. First, we compared the cell growth curve of the LNX1<sup>WT</sup> overexpressed or knockdown cells to that of control cells. As shown in Figure 6C, LNX1 suppression by siLNX1 correlated with significantly faster growth rate, while the LNX1<sup>WT</sup>-overexpressed cells, in which the endogenous PBK was significantly reduced (Figure 6B) ( $p < 0.05$  for 3 independent experiments) (all the raw data was shown in Supplementary Table 17), were significantly less viable than the control cells (Figure 6D), consistent with the elongated population doubling time and slower growth of the stable PBK knockdown cell lines.<sup>50</sup> Second, we examined cell apoptosis of

the LNX1<sup>WT</sup> overexpressed or knockdown cells after treatment with the genotoxin doxorubicin or dimethyl sulfoxide (DMSO). As shown in Figure 6E, LNX1 depletion prompted a significantly decrease in cell death after exposure to doxorubicin. In LNX1<sup>WT</sup>-overexpressed cells, cell apoptosis was significantly increased after exposure to doxorubicin, whereas there was no significant difference in cell apoptosis after exposure to DMSO (Figure 6F). This is also consistent with the phenotypic changes of the stable PBK knockdown cell lines.<sup>50</sup> These results suggest that LNX1-mediated ubiquitination and degradation of PBK inhibited cell proliferation and enhanced sensitivity to doxorubicin-induced apoptosis.

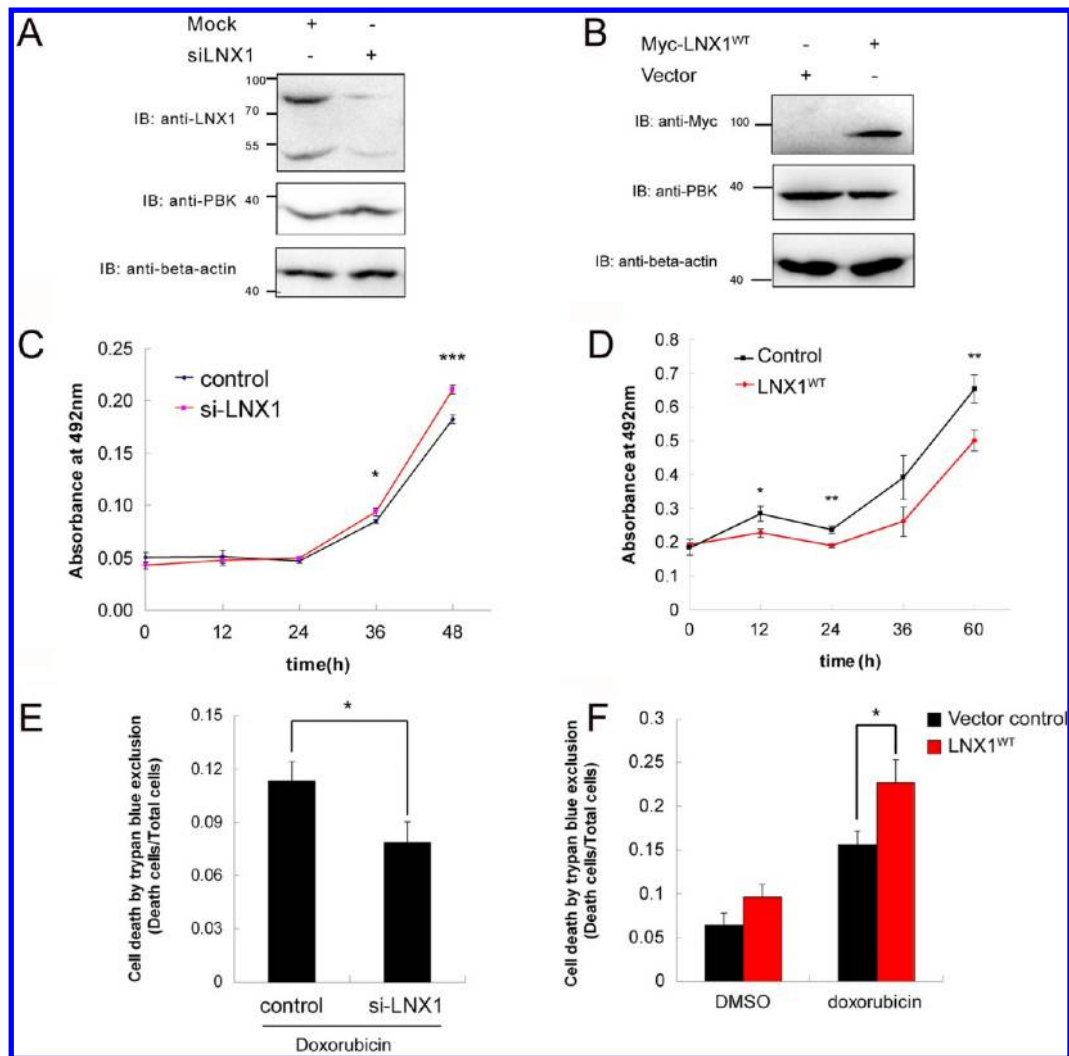


**Figure 6.** Physiological significance of the PBK-LNX1 E3 partnership. (A) siLNK1 (LNX1-specific siRNA) and siNEG.2 (negative control) were transfected into HEK293T cells. The cell lysates were separated by SDS-PAGE and immunoblotted with anti-LNX1 and anti-PBK antibodies. Beta-actin was used as the loading control. Two bands from endogenous LNX1 were detected. Both LNX1 bands were efficiently decreased when siLNK1 was transfected, while the expression of endogenous PBK was enhanced. (B) Western blot analysis of LNX1<sup>WT</sup>-pcDNA4-overexpressed MCF-7 cells and pcDNA4 vector-transfected control MCF-7 cells with anti-PBK and anti-Myc antibodies. Beta-actin was used as the loading control. Overexpressed Myc-tagged LNX1 E3 promoted the down-regulation of endogenous PBK. (C) siLNK1 and siNEG.2 (negative control) were transfected into HEK293T cells. Twenty-four hours after transfection, the 96-well microtiter plates were seeded with  $5 \times 10^5$  cells per well. Next, cell growth was monitored using the MTS method at 0 h, 12 h, 24 h, 36 and 48 h. The averages and S.E.M.s from nine independent wells are shown. (D) LNX1<sup>WT</sup>-pcDNA4 and pcDNA4 (vector control) were transfected into MCF-7 cells, respectively. Twelve hours after transfection, 200  $\mu\text{g}/\text{mL}$  Zeocin was added to select the transfected cells. Twenty-four hours after transfection, the 96-well microtiter plates were seeded with  $1 \times 10^4$  cells per well. Next, cell growth was monitored using the MTS method at 0 h, 12 h, 24 h, 36 and 60 h. The averages and S.E.M.s from nine independent wells are shown. (E) HEK293T cells or (F) MCF-7 cells treated with 1  $\mu\text{M}$  doxorubicin or solvent DMSO were collected and stained with Trypan blue. The number of living cells and dead cells were counted using a hemocytometer. The averages and S.E.M.s from six independent experiments are shown.

### 7. Gene Ontology (GO) Term Enrichment Analysis of LNX1 Ligand Proteins

The possible functions of LNX1 were further explored by analyzing the major functions of its ligands. The PANTHER classification system<sup>35</sup> was used to search for statistical enrichment of the GO terms in 172 LNX1 ligand genes (Supplementary Table 18, Supporting Information), including 50 newly discovered genes, 15 known genes, and 107 potential genes identified from high-throughput interaction screens, comparing to the entire human genome.

One-hundred fifty-seven of the 172 LNX1 ligand genes were classified into molecular function, biological process, and protein class categories for human genes (Figure 7; all the original data

are provided in Supplementary Table 18, Supporting Information). In the molecular function category, LNX1 ligands showed an enrichment of receptor activity and ion channel activity whereas an underrepresentation of transcription regulator activity relative to the entire human genome. In the biological process category, the reproduction term was overrepresented in the LNX1 ligands, whereas the response to stimulus term was underrepresented. In the protein class category, four GO terms (cell junction protein, kinase, isomerase, and transferase) were overrepresented, whereas two terms (transcription factor and hydrolase) were underrepresented. These results suggest that LNX1 is more likely to function in the cytoplasm than in the nucleus. Apparently, LNX1 tend to interact with the membrane or cytosolic proteins, such as receptors, ion channels, cell

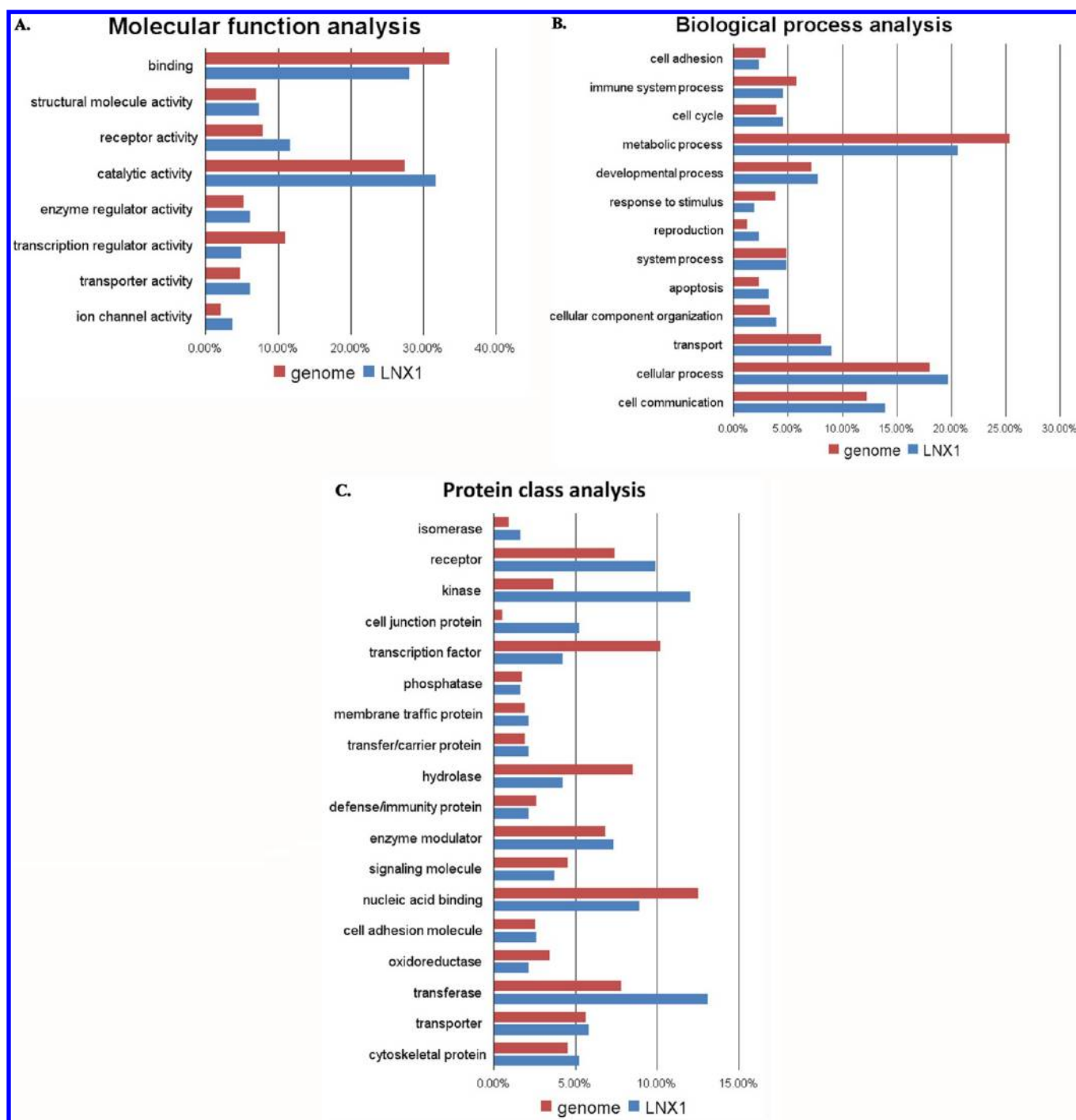


**Figure 7.** GO term enrichment analysis of LNX1 ligand proteins. One hundred and fifty-seven of the 172 LNX1 ligand genes were classified into (A) molecular function, (B) biological process, and (C) protein class categories for human genes, comparing to the entire human genome. Genes for which no annotations could be assigned were excluded from the analysis for both the ligands and the genome set. Categories with at least three genes are displayed in the bar charts.

junction proteins, kinases, isomerases, and transferases, and act as an E3 ligase or a molecular scaffold in regulating the activity, stability, or subcellular localization of its interactors. This proposal is partially supported by previous findings<sup>22</sup> and by our immunofluorescence results (Supplementary Figure 4), which demonstrated that LNX1 was localized in the cytoplasm and was absent in the nucleus.

## DISCUSSION

We developed a proteomics strategy to identify the substrates of E3 ubiquitin ligases that contain protein interaction domains. This strategy is notably different from other approaches in the following respects. First, comprehensive potential ligands, including transient, weak, low-abundant, and even unnatural ligands, can all be identified on a proteomic scale in theory without being restricted to a particular state or cell type. This is because the candidate ligand proteins were predicted by protein

database searches with consensus binding sequences, which were characterized by screenings of random peptide libraries. Second, not only the substrates but also the detailed substrate recognition mechanisms can be characterized. In particular, the domains that are responsible for recognition in E3s and the target sites in the substrates can be specified. Third, not only the substrates but also the nonsubstrate interactors, which are potential regulators of E3s, can be discovered. It is possible that not all of the identified binding partners of LNX PDZ domains act as substrates of LNXs, and nonsubstrate interactors may participate in regulating the ligase activity and subcellular localization of LNXs. Fourth, the whole strategy is simple and efficient. The expression and purification of numerous candidate proteins were unnecessary; thus, the membrane proteins and unstable substrates were more likely to be captured. Because the C-termini of the artificial degrons can be conveniently replaced with different C-terminal sequences of candidate ligands for the *in vitro* ubiquitination assays, the labor and cost for cloning, expressing and purifying full-length candidate substrates can be greatly reduced, thus extending the *in vitro* assay to a larger scale.

This strategy also has several limitations. First, substrates that are independent of interaction with E3s cannot be detected. Second, due to the limitations of the Y2H system, substrates that require their post-translational modifications to be recognized by E3s cannot be discovered, for example, some cullin-RING ligase substrates that typically must be modified, often by phosphorylation.<sup>2</sup> Similarly, substrates that require adapter(s) or cofactor(s) to be recognized by E3s cannot be detected either. The latter two limitations may be overcome by applying the yeast three-hybrid system, in which an exogenous kinase can be used to phosphorylate the Tyr residues on the targets<sup>55</sup> or an exogenous adapter can be introduced to bridge indirect interactions.<sup>56</sup>

In this study, we demonstrated the feasibility of the strategy by employing it to investigate the substrates of the LNX family of E3s. A series of novel interactors of each LNX PDZ domain was identified (Table 2). Among them, six candidates (highlighted in Table 2) had previously been determined to be physiological substrates or interactors of LNX by other independent laboratories,<sup>19,25,27,28,47</sup> and two candidates, PBK and BCR, were validated to be endogenous substrates of LNX1 in mammalian cells in this study. These results not only indicate that other candidates listed in Table 2 have the potential to be physiological substrates or regulators of LNX E3s but also demonstrate the effectiveness of our strategy. However, not all of the known LNX1 interactors were identified in our screen. This likely occurred for several reasons. First, some ligands, such as c-Src, CAST, and RhoC, may be missed in the prediction process because the screening may not be comprehensive and the deduction may not be accurate. Second, the substrates that are recognized by LNX1 but do not interact with just the PDZ domains cannot be identified; Numb, for instance, also requires the PTB-binding motif in LNX1 for recognition.<sup>18</sup> Third, the substrates that are recognized by LNX PDZs via internal peptides but not the C-terminal binding motifs cannot be identified; one example is SKIP, which possesses an unlikely PDZ-binding C-terminal motif, -EGKKRRKE\*.<sup>21</sup> Fourth, some reported ligands, such as the LNX1 self-interaction,<sup>28</sup> were not confirmed in our system. Even the interaction between the full-length LNX1 and its C-terminus was not confirmed in the one-to-one Y2H assay.

LNX1 has been included in several high-throughput interaction screens using different methods, and 107 potential binding proteins were identified<sup>27,29,30</sup> (Supplementary Table 19, Supporting Information). Rual et al. tested all pair wise

interactions of 7194 proteins from the human ORFeome collection in a high-throughput Y2H study.<sup>29</sup> Stiffler et al. identified four interactors for LNX1 PDZ2 in a protein microarray screen of 157 mouse PDZ domains against 217 peptides based on the carboxy termini of mouse proteins.<sup>30</sup> Wolting et al. also used a human protein array to identify LNX1 PDZs binding partners, and 53 potential targets were isolated from 8000 human proteins and 6 novel LNX1 interactors were further confirmed.<sup>27</sup> However, among the 107 potential LNX1 interactors, only PBK and Potassium channel Kv1.4 were identified again in our results. The low overlap between our results and the high-throughput interaction screens might be caused by the different screen methods, including the different binding conditions and the different libraries screened against. We used Y2H method to screen against a random peptide library, whereas Stiffler and Wolting used a protein array screen and Rual et al. screened against a traditional cDNA library in Y2H screen. Additionally, we notice that more than 60% of these 107 potential LNX1 interactors do not have the typical C-terminal PDZ-binding motifs.

LNX1 has previously been reported to function as an E3 ligase<sup>18</sup> or as a molecular scaffold<sup>28</sup> and is involved in several different biological processes, including Notch signaling,<sup>18,57</sup> neuregulin-1/ErbB signaling,<sup>20</sup> cell junction reorganization,<sup>22,25</sup> and human tumorigenesis.<sup>21,24,57</sup> A global genomic study demonstrated that the down-regulation of LNX1 resulted in cell cycle arrest in the G<sub>0</sub>/G<sub>1</sub> phase.<sup>58</sup> PBK encodes a serine/threonine kinase, belonging to the dual specific mitogen-activated protein kinase (MAPKK) family,<sup>49</sup> and it regulates cell mitosis and DNA repair, resulting in the promotion of cell growth and the prevention of apoptosis.<sup>54</sup> PBK has been linked to the control of many cellular processes, including JNK signaling,<sup>52</sup> ERK signaling,<sup>53,59</sup> p38 signaling<sup>51,60</sup> and p53 signaling pathways,<sup>54,61</sup> and it has been shown to be up-regulated in a variety of tumors, such as hematologic malignancies,<sup>62,63</sup> breast cancer,<sup>50,64</sup> and colorectal cancer.<sup>53</sup> In this work, we found that LNX1 mediated-ubiquitination and degradation of PBK inhibited cell proliferation (Figure 6C and D) and enhanced cell sensitivity to doxorubicin-induced apoptosis (Figure 6E and F). This finding demonstrates that LNX1 regulates cell growth and apoptosis and suggests that it may act as a tumor suppressor. Additionally, several previous studies have reported the similar results. LNX1 mutations were found in a subset of human gliomas,<sup>65</sup> and LNX1 was down-regulated in 100% of gliomas.<sup>21</sup> It is also associated with proto-oncogene Np9<sup>57</sup> and c-Src,<sup>24</sup> thereby contributing to tumorigenesis. Therefore, LNX1 should be considered as a previously unappreciated tumor suppressor gene. In addition to PBK, there are another 58 novel LNX binding partners that were identified in this work, and the functions of their interactions with LNX E3 are also worth investigating in the future.

Some PDZ domains have been reported to create functional diversity through the formation of PDZ–PDZ dimerization<sup>66,67</sup> or recognition of internal sequences.<sup>68,69</sup> In this study, LNX1 PDZ4, LNX2 PDZ4 (which retrieved no positive binding ligands in the screenings), and LNX2 PDZ1 (which exhibited no consensus among the positive binding sequences) were revealed to be capable of interacting with other LNX PDZ domains (Figure 2F). Two pairs of LNX PDZ–PDZ interactions, among four PDZ domains, were clearly identified. These interactions potentially act in the following two ways: (1) intramolecular interactions, between PDZ1 and PDZ4 in LNX1 or LNX2; (2) homodimer of LNX1 or LNX2. The PDZ–PDZ interactions

may regulate substrate recognition and the strength of substrate ubiquitination. This speculation can be supported by a previous report in which Numb was shown to be more strongly ubiquitinated by LNX1 without PDZ4 than by the full-length LNX1.<sup>18</sup> The same phenomenon was also referenced for another LNX1 substrate, c-Src.<sup>24</sup> The PDZ–PDZ interactions may also promote the formation of a LNX multimolecular oligomer that serves as a molecular scaffold.

This strategy can be potentially extended to a variety of E3s that contain protein interaction domain(s), as long as the ligands of the interaction domains can be identified by screening a random peptide library, such as SH3,<sup>70–77</sup> WW,<sup>78</sup> and GYF,<sup>79</sup> whose binding properties have been successfully characterized by screening a phage-displayed random peptide library. In fact, at least three-quarters of RING-type<sup>2</sup> and numerous HECT-type single-subunit E3s, which have PDZ, WW, SH3 or other interaction domains,<sup>2,13,80</sup> can be analyzed using our strategy. For the multisubunit E3 complexes in which the ubiquitin ligase domain and substrate recognition domain are separated into discrete subunits, our strategy can also be used by screening with the recognition domain as the bait to identify the candidates.

## ■ ASSOCIATED CONTENT

### Supporting Information

Supplementary information as detailed in text. This material is available free of charge via the Internet at <http://pubs.acs.org>.

## ■ AUTHOR INFORMATION

### Corresponding Author

\*Youhe Gao, Tel: 86-10-6529-6407. Fax: 86-10-6521-2284. E-mail: [gaoyouhe@pumc.edu.cn](mailto:gaoyouhe@pumc.edu.cn). Eli Song, Tel: 86-10-6488-8522. Fax: 86-10-6488-8524. E-mail: [songali@moon.ibp.ac.cn](mailto:songali@moon.ibp.ac.cn).

### Author Contributions

‡These authors contributed equally to this work.

### Notes

The authors declare no competing financial interest.

## ■ ACKNOWLEDGMENTS

We thank Dr. Huihua Li for kindly providing the ubiquitin plasmids and Dr. Chengyu Jiang for kindly providing the HEK293ET cell line. This work was supported by the National Basic Research Program of China (2012CB517606, 2011CB964901), National Natural Science Foundation (30900268, 31270884, 31200614), the Beijing Natural Science Foundation (S092017, S122026), the National High Technology Research and Development Program of China (2011AA020116), Program for Changjiang Scholars and Innovative Research Team in University-PCSIRT (IRT0909), and 111 Project (B08007).

## ■ ABBREVIATIONS

AD, activation domain; BD, binding domain; Degron, degradation signal; E1, ubiquitin activating enzyme; E2, ubiquitin conjugating enzyme; E3, ubiquitin ligase; GO, Gene Ontology; HECT, homologous to the E6-AP carboxyl terminus; IPTG, isopropyl  $\beta$ -D-1-thiogalactopyranoside; LNX, Ligand of Numb protein X; MG132, Z-Leu-Leu-Leu-al; MTS, 3-(4,5-dimethylthiazol-2-yl)-5-(3-carboxymethoxyphenyl)-2-(4-sulfo-phenyl)-2H-tetrazolium, inner salt; PDZ domain, PSD-95/SAP90, DLG and ZO-1 domain; RING, really interesting new

gene; SPOT synthesis, synthesis of peptides on cellulose membranes; Ub, ubiquitin; Y2H, yeast two-hybrid.

## ■ REFERENCES

- (1) Lu, J. Y.; Lin, Y. Y.; Qian, J.; Tao, S. C.; Zhu, J.; Pickart, C.; Zhu, H. Functional dissection of a HECT ubiquitin E3 ligase. *Mol. Cell. Proteomics* **2008**, *7*, 35–45.
- (2) Deshaies, R. J.; Joazeiro, C. A. RING domain E3 ubiquitin ligases. *Annu. Rev. Biochem.* **2009**, *78*, 399–434.
- (3) Ciechanover, A.; Heller, H.; Elias, S.; Haas, A. L.; Hershko, A. ATP dependent conjugation of reticulocyte proteins with the polypeptide required for protein degradation. *Proc. Natl. Acad. Sci. U.S.A.* **1980**, *77*, 1365–1368.
- (4) Hershko, A.; Ciechanover, A.; Heller, H.; Haas, A. L.; Rose, I. A. Proposed role of ATP in protein breakdown: conjugation of protein with multiple chains of the polypeptide of ATP-dependent proteolysis. *Proc. Natl. Acad. Sci. U.S.A.* **1980**, *77*, 1783–1786.
- (5) Hershko, A.; Heller, H.; Elias, S.; Ciechanover, A. Components of ubiquitin-protein ligase system. Resolution, affinity purification, and role in protein breakdown. *J. Biol. Chem.* **1983**, *258*, 8206–8214.
- (6) Hershko, A.; Ciechanover, A. The ubiquitin system. *Annu. Rev. Biochem.* **1998**, *67*, 425–479.
- (7) Pickart, C. M. Mechanisms underlying ubiquitination. *Annu. Rev. Biochem.* **2001**, *70*, 503–533.
- (8) Robinson, P. A.; Ardley, H. C. Ubiquitin-protein ligases—novel therapeutic targets? *Curr. Protein Pept. Sci.* **2004**, *5*, 163–176.
- (9) Gupta, R.; Kus, B.; Fladd, C.; Wasmuth, J.; Tonikian, R.; Sidhu, S.; Krogan, N. J.; Parkinson, J.; Rotin, D. Ubiquitination screen using protein microarrays for comprehensive identification of Rsp5 substrates in yeast. *Mol. Syst. Biol.* **2007**, *3*, 116.
- (10) Persaud, A.; Alberts, P.; Amsen, E. M.; Xiong, X.; Wasmuth, J.; Saadon, Z.; Fladd, C.; Parkinson, J.; Rotin, D. Comparison of substrate specificity of the ubiquitin ligases Nedd4 and Nedd4–2 using proteome arrays. *Mol. Syst. Biol.* **2009**, *5*, 333.
- (11) Burande, C. F.; Heuze, M. L.; Lamsoul, I.; Monsarrat, B.; Uttenweiler-Joseph, S.; Lutz, P. G. A label-free quantitative proteomics strategy to identify E3 ubiquitin ligase substrates targeted to proteasome degradation. *Mol. Cell. Proteomics* **2009**, *8*, 1719–1727.
- (12) Sun, W.; Wu, S.; Wang, X.; Zheng, D.; Gao, Y. An analysis of protein abundance suppression in data dependent liquid chromatography and tandem mass spectrometry with tryptic peptide mixtures of five known proteins. *Eur. J. Mass Spectrom.* **2005**, *11*, 575–580.
- (13) Li, W.; Bengtson, M. H.; Ulbrich, A.; Matsuda, A.; Reddy, V. A.; Orth, A.; Chanda, S. K.; Batalov, S.; Joazeiro, C. A. Genome-wide and functional annotation of human E3 ubiquitin ligases identifies MULAN, a mitochondrial E3 that regulates the organelle's dynamics and signaling. *PLoS One* **2008**, *3*, e1487.
- (14) Weissman, A. M. Themes and variations on ubiquitylation. *Nat. Rev. Mol. Cell. Biol.* **2001**, *2*, 169–178.
- (15) Songyang, Z.; Fanning, A. S.; Fu, C.; Xu, J.; Marfatia, S. M.; Chishti, A. H.; Crompton, A.; Chan, A. C.; Anderson, J. M.; Cantley, L. C. Recognition of unique carboxyl-terminal motifs by distinct PDZ domains. *Science* **1997**, *275*, 73–77.
- (16) Kim, E.; Sheng, M. PDZ domain proteins of synapses. *Nat. Rev. Neurosci.* **2004**, *5*, 771–781.
- (17) Dho, S. E.; Jacob, S.; Wolting, C. D.; French, M. B.; Rohrschneider, L. R.; McGlade, C. J. The mammalian numb phosphotyrosine-binding domain. Characterization of binding specificity and identification of a novel PDZ domain-containing numb binding protein, LNX. *J. Biol. Chem.* **1998**, *273*, 9179–9187.
- (18) Nie, J.; McGill, M. A.; Dermer, M.; Dho, S. E.; Wolting, C. D.; McGlade, C. J. LNX functions as a RING type E3 ubiquitin ligase that targets the cell fate determinant Numb for ubiquitin-dependent degradation. *EMBO J.* **2002**, *21*, 93–102.
- (19) Sollerbrant, K.; Raschperger, E.; Mirza, M.; Engstrom, U.; Philipson, L.; Ljungdahl, P. O.; Pettersson, R. F. The Coxsackievirus and adenovirus receptor (CAR) forms a complex with the PDZ domain-containing protein ligand-of-numb protein-X (LNX). *J. Biol. Chem.* **2003**, *278*, 7439–7444.

- (20) Young, P.; Nie, J.; Wang, X.; McGlade, C. J.; Rich, M. M.; Feng, G. LNX1 is a perisynaptic Schwann cell specific E3 ubiquitin ligase that interacts with ErbB2. *Mol. Cell. Neurosci.* **2005**, *30*, 238–248.
- (21) Chen, J.; Xu, J.; Zhao, W.; Hu, G.; Cheng, H.; Kang, Y.; Xie, Y.; Lu, Y. Characterization of human LNX, a novel ligand of Numb protein X that is downregulated in human gliomas. *Int. J. Biochem. Cell Biol.* **2005**, *37*, 2273–2283.
- (22) Kansaku, A.; Hirabayashi, S.; Mori, H.; Fujiwara, N.; Kawata, A.; Ikeda, M.; Rokukawa, C.; Kurihara, H.; Hata, Y. Ligand-of-Numb protein X is an endocytic scaffold for junctional adhesion molecule 4. *Oncogene* **2006**, *25*, 5071–5084.
- (23) Higa, S.; Tokoro, T.; Inoue, E.; Kitajima, I.; Ohtsuka, T. The active zone protein CAST directly associates with Ligand-of-Numb protein X. *Biochem. Biophys. Res. Commun.* **2007**, *354*, 686–692.
- (24) Weiss, A.; Baumgartner, M.; Radziwill, G.; Dennler, J.; Moelling, K. c-Src is a PDZ interaction partner and substrate of the E3 ubiquitin ligase Ligand-of-Numb protein X1. *FEBS Lett.* **2007**, *581*, 5131–5136.
- (25) Takahashi, S.; Iwamoto, N.; Sasaki, H.; Ohashi, M.; Oda, Y.; Tsukita, S.; Furuse, M. The E3 ubiquitin ligase LNX1p80 promotes the removal of claudins from tight junctions in MDCK cells. *J. Cell Sci.* **2009**, *122*, 985–994.
- (26) Zheng, D.; Sun, Y.; Gu, S.; Ji, C.; Zhao, W.; Xie, Y.; Mao, Y. LNX (Ligand of Numb-protein X) interacts with RhoC, both of which regulate AP-1-mediated transcriptional activation. *Mol. Biol. Rep.* **2010**, *37*, 2431–2437.
- (27) Wolting, C. D.; Griffiths, E. K.; Sarao, R.; Prevost, B. C.; Wybenga-Groot, L. E.; McGlade, C. J. Biochemical and computational analysis of LNX1 interacting proteins. *PLoS One* **2011**, *6*, e26248.
- (28) Rice, D. S.; Northcutt, G. M.; Kurschner, C. The Lnx family proteins function as molecular scaffolds for Numb family proteins. *Mol. Cell. Neurosci.* **2001**, *18*, 525–540.
- (29) Rual, J. F.; Venkatesan, K.; Hao, T.; Hirozane-Kishikawa, T.; Dricot, A.; Li, N.; Berriz, G. F.; Gibbons, F. D.; Dreze, M.; Ayivi-Guedehoussou, N.; Klitgord, N.; Simon, C.; Boxem, M.; Milstein, S.; Rosenberg, J.; Goldberg, D. S.; Zhang, L. V.; Wong, S. L.; Franklin, G.; Li, S.; Albal, J. S.; Lim, J.; Fraughton, C.; Llamosas, E.; Cevik, S.; Bex, C.; Lamesch, P.; Sikorski, R. S.; Vandenhaute, J.; Zoghbi, H. Y.; Smolyar, A.; Bosak, S.; Sequerra, R.; Doucette-Stamm, L.; Cusick, M. E.; Hill, D. E.; Roth, F. P.; Vidal, M. Towards a proteome-scale map of the human protein-protein interaction network. *Nature* **2005**, *437*, 1173–1178.
- (30) Stiffler, M. A.; Chen, J. R.; Grantcharova, V. P.; Lei, Y.; Fuchs, D.; Allen, J. E.; Zaslavskaja, L. A.; MacBeath, G. PDZ domain binding selectivity is optimized across the mouse proteome. *Science* **2007**, *317*, 364–369.
- (31) Nie, J.; Li, S. S.; McGlade, C. J. A novel PTB-PDZ domain interaction mediates isoform-specific ubiquitylation of mammalian Numb. *J. Biol. Chem.* **2004**, *279*, 20807–20815.
- (32) Song, E.; Gao, S.; Tian, R.; Ma, S.; Huang, H.; Guo, J.; Li, Y.; Zhang, L.; Gao, Y. A high efficiency strategy for binding property characterization of peptide-binding domains. *Mol. Cell. Proteomics.* **2006**, *5*, 1368–1381.
- (33) Ma, S.; Song, E.; Gao, S.; Tian, R.; Gao, Y. Rapid characterization of the binding property of HtrA2/Omi PDZ domain by validation screening of PDZ ligand library. *Sci. China C Life Sci.* **2007**, *50*, 412–422.
- (34) Crooks, G. E.; Hon, G.; Chandonia, J. M.; Brenner, S. E. WebLogo: a sequence logo generator. *Genome Res.* **2004**, *14*, 1188–1190.
- (35) Mi, H.; Lazareva-Ulitsky, B.; Loo, R.; Kejariwal, A.; Vandergriff, J.; Rabkin, S.; Guo, N.; Muruganujan, A.; Doremioux, O.; Campbell, M. J.; Kitano, H.; Thomas, P. D. The PANTHER database of protein families, subfamilies, functions and pathways. *Nucleic Acids Res.* **2005**, *33*, D284–288.
- (36) Ju, D.; Xie, Y. Identification of the preferential ubiquitination site and ubiquitin-dependent degradation signal of Rpn4. *J. Biol. Chem.* **2006**, *281*, 10657–10662.
- (37) Marengere, L. E.; Songyang, Z.; Gish, G. D.; Schaller, M. D.; Parsons, J. T.; Stern, M. J.; Cantley, L. C.; Pawson, T. SH2 domain specificity and activity modified by a single residue. *Nature* **1994**, *369*, 502–505.
- (38) Rodriguez, M.; Li, S. S.; Harper, J. W.; Songyang, Z. An oriented peptide array library (OPAL) strategy to study protein-protein interactions. *J. Biol. Chem.* **2004**, *279*, 8802–8807.
- (39) Boisguerin, P.; Leben, R.; Ay, B.; Radziwill, G.; Moelling, K.; Dong, L.; Volkmer-Engert, R. An improved method for the synthesis of cellulose membrane-bound peptides with free C termini is useful for PDZ domain binding studies. *Chem. Biol.* **2004**, *11*, 449–459.
- (40) Vaccaro, P.; Brannetti, B.; Montecchi-Palazzi, L.; Philipp, S.; Helmer Citterich, M.; Cesareni, G.; Dente, L. Distinct binding specificity of the multiple PDZ domains of INADL, a human protein with homology to INAD from *Drosophila melanogaster*. *J. Biol. Chem.* **2001**, *276*, 42122–42130.
- (41) Fields, S.; Song, O. A novel genetic system to detect protein-protein interactions. *Nature* **1989**, *340*, 245–246.
- (42) Jelen, F.; Oleksy, A.; Smietana, K.; Otlewski, J. PDZ domains - common players in the cell signaling. *Acta Biochim. Pol.* **2003**, *50*, 985–1017.
- (43) Bezprozvanny, I.; Maximov, A. Classification of PDZ domains. *FEBS Lett.* **2001**, *509*, 457–462.
- (44) Schneider, S.; Buchert, M.; Georgiev, O.; Catimel, B.; Halford, M.; Stacker, S. A.; Baechi, T.; Moelling, K.; Hovens, C. M. Mutagenesis and selection of PDZ domains that bind new protein targets. *Nat. Biotechnol.* **1999**, *17*, 170–175.
- (45) Tonikian, R.; Zhang, Y.; Sazinsky, S. L.; Currell, B.; Yeh, J. H.; Reva, B.; Held, H. A.; Appleton, B. A.; Evangelista, M.; Wu, Y.; Xin, X.; Chan, A. C.; Seshagiri, S.; Lasky, L. A.; Sander, C.; Boone, C.; Bader, G. D.; Sidhu, S. S. A specificity map for the PDZ domain family. *PLoS Biol.* **2008**, *6*, e239.
- (46) Huang, H. M.; Zhang, L.; Cui, Q. H.; Jiang, T. Z.; Ma, S. C.; Gao, Y. H. Finding potential ligands for PDZ domains by tailfit, a JAVA program. *Chin. Med. Sci. J.* **2004**, *19*, 97–104.
- (47) Mirza, M.; Raschperger, E.; Philipson, L.; Pettersson, R. F.; Sollerbrant, K. The cell surface protein coxsackie- and adenovirus receptor (CAR) directly associates with the Ligand-of-Numb Protein-X2 (LNX2). *Exp. Cell Res.* **2005**, *309*, 110–120.
- (48) Ravid, T.; Hochstrasser, M. Diversity of degradation signals in the ubiquitin-proteasome system. *Nat. Rev. Mol. Cell. Biol.* **2008**, *9*, 679–690.
- (49) Gaudet, S.; Branton, D.; Lue, R. A. Characterization of PDZ-binding kinase, a mitotic kinase. *Proc. Natl. Acad. Sci. U.S.A.* **2000**, *97*, 5167–5172.
- (50) Park, J. H.; Lin, M. L.; Nishidate, T.; Nakamura, Y.; Katagiri, T. PDZ-binding kinase/T-LAK cell-originated protein kinase, a putative cancer/testis antigen with an oncogenic activity in breast cancer. *Cancer Res.* **2006**, *66*, 9186–9195.
- (51) Ayllon, V.; O'Connor, R. PBK/TOPK promotes tumour cell proliferation through p38 MAPK activity and regulation of the DNA damage response. *Oncogene* **2007**, *26*, 3451–3461.
- (52) Oh, S. M.; Zhu, F.; Cho, Y. Y.; Lee, K. W.; Kang, B. S.; Kim, H. G.; Zykova, T.; Bode, A. M.; Dong, Z. T-lymphokine-activated killer cell-originated protein kinase functions as a positive regulator of c-Jun-NH2-kinase 1 signaling and H-Ras-induced cell transformation. *Cancer Res.* **2007**, *67*, 5186–5194.
- (53) Zhu, F.; Zykova, T. A.; Kang, B. S.; Wang, Z.; Ebeling, M. C.; Abe, Y.; Ma, W. Y.; Bode, A. M.; Dong, Z. Bidirectional signals transduced by TOPK-ERK interaction increase tumorigenesis of HCT116 colorectal cancer cells. *Gastroenterology* **2007**, *133*, 219–231.
- (54) Hu, F.; Gartenhaus, R. B.; Eichberg, D.; Liu, Z.; Fang, H. B.; Rapoport, A. P. PBK/TOPK interacts with the DBD domain of tumor suppressor p53 and modulates expression of transcriptional targets including p21. *Oncogene* **2010**, *29*, 5464–5474.
- (55) Osborne, M. A.; Dalton, S.; Kochan, J. P. The yeast tribrid system—genetic detection of trans-phosphorylated ITAM-SH2-interactions. *Biotechnology* **1995**, *13*, 1474–1478.
- (56) Zhang, J.; Lautar, S. A yeast three-hybrid method to clone ternary protein complex components. *Anal. Biochem.* **1996**, *242*, 68–72.
- (57) Armbruster, V.; Sauter, M.; Roemer, K.; Best, B.; Hahn, S.; Nty, A.; Schmid, A.; Philipp, S.; Mueller, A.; Mueller-Lantzsch, N. Np9

protein of human endogenous retrovirus K interacts with ligand of numb protein X. *J. Virol.* **2004**, *78*, 10310–10319.

(58) Zheng, D.; Gu, S.; Li, Y.; Ji, C.; Xie, Y.; Mao, Y. A global genomic view on LNX siRNA-mediated cell cycle arrest. *Mol. Biol. Rep.* **2011**, *38*, 2771–2783.

(59) Aksamitiene, E.; Kholodenko, B. N.; Kolch, W.; Hoek, J. B.; Kiyatkin, A. PI3K/Akt-sensitive MEK-independent compensatory circuit of ERK activation in ER-positive PI3K-mutant T47D breast cancer cells. *Cell Signal.* **2010**, *22*, 1369–1378.

(60) Li, S.; Zhu, F.; Zykova, T.; Kim, M. O.; Cho, Y. Y.; Bode, A. M.; Peng, C.; Ma, W.; Carper, A.; Langfald, A.; Dong, Z. T-LAK cell-originated protein kinase (TOPK) phosphorylation of MKP1 protein prevents solar ultraviolet light-induced inflammation through inhibition of the p38 protein signaling pathway. *J. Biol. Chem.* **2011**, *286*, 29601–29609.

(61) Nandi, A. K.; Ford, T.; Fleksher, D.; Neuman, B.; Rapoport, A. P. Attenuation of DNA damage checkpoint by PBK, a novel mitotic kinase, involves protein-protein interaction with tumor suppressor p53. *Biochem. Biophys. Res. Commun.* **2007**, *358*, 181–188.

(62) Simons-Evelyn, M.; Bailey-Dell, K.; Toretsky, J. A.; Ross, D. D.; Fenton, R.; Kalvakolanu, D.; Rapoport, A. P. PBK/TOPK is a novel mitotic kinase which is upregulated in Burkitt's lymphoma and other highly proliferative malignant cells. *Blood Cells Mol. Dis.* **2001**, *27*, 825–829.

(63) Nandi, A.; Tidwell, M.; Karp, J.; Rapoport, A. P. Protein expression of PDZ-binding kinase is up-regulated in hematologic malignancies and strongly down-regulated during terminal differentiation of HL-60 leukemic cells. *Blood Cells Mol. Dis.* **2004**, *32*, 240–245.

(64) Fukukawa, C.; Ueda, K.; Nishidate, T.; Katagiri, T.; Nakamura, Y. Critical roles of LGN/GPSM2 phosphorylation by PBK/TOPK in cell division of breast cancer cells. *Genes Chromosomes Cancer* **2010**, *49*, 861–872.

(65) Blom, T.; Roselli, A.; Tanner, M.; Nupponen, N. N. Mutation and copy number analysis of LNX1 and Numbl in nervous system tumors. *Cancer Genet. Cytogenet.* **2008**, *186*, 103–109.

(66) Im, Y. J.; Lee, J. H.; Park, S. H.; Park, S. J.; Rho, S. H.; Kang, G. B.; Kim, E.; Eom, S. H. Crystal structure of the Shank PDZ-ligand complex reveals a class I PDZ interaction and a novel PDZ-PDZ dimerization. *J. Biol. Chem.* **2003**, *278*, 48099–48104.

(67) Nourry, C.; Grant, S. G.; Borg, J. P. PDZ domain proteins: plug and play! *Sci. STKE* **2003**, *2003*, RE7.

(68) Penkert, R. R.; DiVittorio, H. M.; Prehoda, K. E. Internal recognition through PDZ domain plasticity in the Par-6-Pals1 complex. *Nat. Struct. Mol. Biol.* **2004**, *11*, 1122–1127.

(69) Wong, H. C.; Bourdelas, A.; Krauss, A.; Lee, H. J.; Shao, Y.; Wu, D.; Mlodzik, M.; Shi, D. L.; Zheng, J. Direct binding of the PDZ domain of Dishevelled to a conserved internal sequence in the C-terminal region of Frizzled. *Mol. Cell* **2003**, *12*, 1251–1260.

(70) Sparks, A. B.; Rider, J. E.; Kay, B. K. Mapping the specificity of SH3 domains with phage-displayed random-peptide libraries. *Methods Mol. Biol.* **1998**, *84*, 87–103.

(71) Sparks, A. B.; Rider, J. E.; Hoffman, N. G.; Fowlkes, D. M.; Quilliam, L. A.; Kay, B. K. Distinct ligand preferences of Src homology 3 domains from Src, Yes, Abl, Cortactin, p53bp2, PLCgamma, Crk, and Grb2. *Proc. Natl. Acad. Sci. U.S.A.* **1996**, *93*, 1540–1544.

(72) Rickles, R. J.; Botfield, M. C.; Weng, Z.; Taylor, J. A.; Green, O. M.; Brugge, J. S.; Zoller, M. J. Identification of Src, Fyn, Lyn, PI3K and Abl SH3 domain ligands using phage display libraries. *EMBO J.* **1994**, *13*, 5598–5604.

(73) Cheadle, C.; Ivashchenko, Y.; South, V.; Searfoss, G. H.; French, S.; Howk, R.; Ricca, G. A.; Jaye, M. Identification of a Src SH3 domain binding motif by screening a random phage display library. *J. Biol. Chem.* **1994**, *269*, 24034–24039.

(74) Hoffman, N. G.; Sparks, A. B.; Carter, J. M.; Kay, B. K. Binding properties of SH3 peptide ligands identified from phage-displayed random peptide libraries. *Mol. Divers.* **1996**, *2*, 5–12.

(75) Sparks, A. B.; Adey, N. B.; Quilliam, L. A.; Thorn, J. M.; Kay, B. K. Screening phage-displayed random peptide libraries for SH3 ligands. *Methods Enzymol.* **1995**, *255*, 498–509.

(76) Sparks, A. B.; Quilliam, L. A.; Thorn, J. M.; Der, C. J.; Kay, B. K. Identification and characterization of Src SH3 ligands from phage-displayed random peptide libraries. *J. Biol. Chem.* **1994**, *269*, 23853–23856.

(77) Tong, A. H.; Drees, B.; Nardelli, G.; Bader, G. D.; Brannetti, B.; Castagnoli, L.; Evangelista, M.; Ferracuti, S.; Nelson, B.; Paoluzi, S.; Quondam, M.; Zucconi, A.; Hogue, C. W.; Fields, S.; Boone, C.; Cesareni, G. A combined experimental and computational strategy to define protein interaction networks for peptide recognition modules. *Science* **2002**, *295*, 321–324.

(78) Kasanov, J.; Pirozzi, G.; Uveges, A. J.; Kay, B. K. Characterizing Class I WW domains defines key specificity determinants and generates mutant domains with novel specificities. *Chem. Biol.* **2001**, *8*, 231–241.

(79) Kofler, M.; Motzny, K.; Freund, C. GYF domain proteomics reveals interaction sites in known and novel target proteins. *Mol. Cell. Proteomics* **2005**, *4*, 1797–1811.

(80) Shearwin-Whyatt, L.; Dalton, H. E.; Foot, N.; Kumar, S. Regulation of functional diversity within the Nedd4 family by accessory and adaptor proteins. *Bioessays* **2006**, *28*, 617–628.